Title

Robust Global Trajectory Tracking for Underactuated VTOL Aerial Vehicles Using Inner-Outer Loop Control Paradigms

Journal

IEEE Transactions on Automatic Control, 62(1)

ISSN

0018-9286

Authors

Naldi, Roberto
Furci, Michele
Sanfelice, Ricardo G
et al.

Publication Date

2017

DOI

10.1109/tac.2016.2557967

Peer reviewed

Robust Global Trajectory Tracking for Underactuated VTOL Aerial Vehicles using Inner-Outer Loop Control Paradigms

Roberto Naldi, Michele Furci, Ricardo G. Sanfelice and Lorenzo Marconi

***Abstract*—This work proposes a feedback control strategy to let the dynamics of a class of under-actuated Vertical Take-Off and Landing (VTOL) aerial vehicle tracking a desired position and attitude trajectory globally with respect to the initial conditions. The proposed feedback controller is derived following an inner-outer loop control paradigm, namely by considering the attitude, which is governed by means of a hybrid controller so as to overcome the well-known topological constraints, serving as a virtual input to stabilize the aircraft position. Two different approaches, the first one obtained by assuming perfect knowledge of the vehicle dynamics and the second one obtained by considering uncertainties and exogenous disturbances, are proposed and compared by analyzing the interconnection between the hybrid attitude and the continuous-time position closed-loop subsystems. The effectiveness of the obtained results is demonstrated by means of simulations and experiments using a miniature quadrotor prototype.**

***Index Terms*—Aerial Robotics, Nonlinear Control, Interconnected Systems, Hybrid Control, Robust Control.**

I. INTRODUCTION

Miniature Vertical Take-Off and Landing (VTOL) aerial systems are currently employed successfully in a large number of applications including, among others, surveillance, aerial photography and search and rescue operations [1]. One reason for this large success is the high level of maneuverability which allows to safely perform flight missions even in densely cluttered environments [2] or even to perform advanced robotic tasks [3]. Among the different configurations, the class of VTOL aerial systems includes helicopters [4], ducted-fan tail-sitters - [5], [6] - and multi-propeller helicopters - [7], [8], [9]. All of these vehicles are under-actuated mechanical systems, namely the number of available control inputs is less than the number of degrees-of-freedom (d.o.f.). As a consequence, to achieve the high level of agility required by real-world applications, the feedback control design plays a central role.

Several contributions - [10], [11], [12], [13] - document different approaches to the control design for such a class of under-actuated systems. In [14], almost-global stability results are demonstrated by means of Lyapunov based techniques. Results therein show robustness also in the presence of aerodynamic drag disturbances that typically affect aerial systems. Trajectory tracking in the absence of linear velocity measurements has been considered in [15] where a hierarchical controller has also been proposed. In [16], almost-global stability results are achieved by considering geometric methods and then applied to the control of a quadrotor aerial vehicle. Backstepping control design has been proposed in [17] in order to perform aggressive maneuvers by considering the dynamics of a model helicopter and in [18] by considering a hybrid controller able to globally stabilize a desired trajectory. In [19] and [20], inner-outer loop control strategies have been employed to stabilize the dynamical model of a miniature helicopter. The proposed methodology takes into account for the feedback interconnection between the inner attitude and the outer position control loops. In particular, nested saturations and high-gain control techniques are used to show stability of the overall closed-loop system under some limitations in term of the initial attitude configuration. More recently, a survey describing feedback control design for under-actuated VTOL systems has appeared in [21].

In this work, hierarchical control strategies for a miniature VTOL vehicle to track a desired trajectory globally with respect to the initial position and attitude configuration are proposed. In particular, drawing inspiration from recent results pertaining to attitude control of rigid bodies [22], hybrid control techniques [23] are used to overcome the topological obstruction affecting continuous-time globally stabilizing control laws [24]. Robustness with respect to possibly large exogenous disturbances and parametric uncertainties is the main contribution. This is achieved by combining total stability tools for nonlinear control systems [25] with a suitable design of the hybrid control law.

Two different hierarchical control approaches are employed and compared. The first approach is based on the idea of "breaking the loop" between the attitude and the position closed-loop dynamics through a suitable choice of the control torques. The overall closed-loop system can be considered as a cascade connection in which the attitude and the position controllers can be tuned independently to achieve the desired stability properties. However, this control design relies upon the perfect knowledge of the vehicle dynamics and then it may not be effective in the general real-world scenario in which uncertainties and disturbances, including wind and

This research has been conducted in part under the collaborative project SHERPA (IP 600958) supported by the European Community under the 7th Framework Programme. Corresponding author: Roberto Naldi, email: roberto.naldi@unibo.it

R. Naldi, M. Furci and L. Marconi are with CASY-DEI, Università di Bologna, Bologna, 40133, Italy, roberto.naldi@unibo.it, michele.furci@unibo.it, lorenzo.marconi@unibo.it. R.G. Sanfelice is with University of California, Santa Cruz, CA 95064 - USA, ricardo@ucsc.edu. Corresponding author: Roberto Naldi, roberto.naldi@unibo.it.

aerodynamic drag forces, affect the dynamics of the vehicle.

To overcome this important limitation, a second approach is proposed. Since the lack of full knowledge of the system dynamics prevents one to compensate the influence of the position dynamics on the attitude of the vehicle, we propose an attitude controller that combines a linear hybrid feedback law and a feed-forward law obtained by nominal model inversion. The resulting control law is more suitable for practical implementation on a real autopilot due to robustness properties. Such a control law, however, leads to a more involved feedback interconnection between the hybrid attitude and the continuous-time position closed-loop subsystems and, in turn, to a more complex closed-loop analysis.

The paper is organized as follows. Section II introduces the notation and the supporting results from the literature of hybrid systems. Section III-A presents the dynamical model for the class of under-actuated aerial vehicles of interest. Section III-B introduces the control problem which is then addressed in Section IV considering both the nominal and the robust cases. Finally, the application of the robust algorithm to the control of a miniature quadrotor prototype is presented in Section V. Both numerical simulations and experiments are presented.

II. Preliminaries

A. Notation and Definitions

Throughout this paper, $\mathcal{F}_i$ and $\mathcal{F}_b$ denote, respectively, an inertial reference frame and a reference frame attached to the center of gravity of the vehicle. With $I_n \in \mathbb{R}^{n\times n}$ we denote the n-dimensional identity matrix. The symbols $\mathbb{R}, \mathbb{R}_>, \mathbb{R}_\geq$ denote the set of real, positive real, and non-negative real numbers, respectively. For $x \in \mathbb{R}^n$, $|x|$ denotes the Euclidean norm and, given a closed set $\mathcal{A} \subset \mathbb{R}^n$, $|x|_\mathcal{A} = \inf_{y\in\mathcal{A}} |x - y|$. For a function $f : [0, \infty) \to \mathbb{R}^k$, $k > 0$, we define with $|f|_\infty := \sup_{t\in[0,\infty)} |f(t)|$ and $|f|_a := \limsup_{t\to\infty} |f(t)|$. Given a set $\mathcal{M}$, $\overline{\mathcal{M}}$ denotes its closure. Given sets $\mathcal{S}_1$ and $\mathcal{S}_2$, the notation $f : \mathcal{S}_1 \rightrightarrows \mathcal{S}_2$ denotes a set-valued map mapping subsets of $\mathcal{S}_1$ onto subsets of $\mathcal{S}_2$. With $\mathcal{B}^n_r$ we denote the closed ball of radius r centered at the origin of $\mathbb{R}^n$, namely $\mathcal{B}^n_r = \{x \in \mathbb{R}^n : |x| \leq r\}$. Given a function $f : \mathbb{R} \to \mathbb{R}$ and $i \in \mathbb{N}$, we use the notation $f(t)^{(i)} := \frac{d^i}{dt^i} f(t)$ to denote derivative of f with respect to t. We denote the unit vectors as $e_1 := [1, 0, 0]^\top$, $e_2 := [0, 1, 0]^\top$, and $e_3 := [0, 0, 1]^\top$. For any $x \in \mathbb{R}^3$, we let $S(x)$ - with the first, second and third rows given by $[0, -x_3, x_2]$, $[x_3, 0, -x_1]$ and $[-x_2, x_1, 0]$ - be a skew-symmetric matrix and we denote with $^\wedge$ the inverse operator such that $S(x)^\wedge = x$. Let $SO(3)$ denote the *special orthogonal group* of order three, i.e., $SO(3) = \{R \in \mathbb{R}^{3\times3} : R^\top R = RR^\top = I_3, \det R = 1\}$. Given a rotation matrix $R \in SO(3)$, $\Theta(R) := \frac{1}{2}\text{trace}(I_3 - R)$. We denote the n-dimensional unit sphere as $\mathbf{S}_n := \{x \in \mathbb{R}^{n+1} : |x| = 1\}$.

A unit quaternion $q \in \mathbf{S}_3$ is defined as a pair $q = [\eta, \epsilon^\top]^\top$ in which $\eta \in \mathbb{R}$ and $\epsilon \in \mathbb{R}^3$ are denoted, respectively, as the scalar and vector part. Given unit quaternions $q_1 = [\eta_1, \epsilon_1^\top]^\top$ and $q_2 = [\eta_2, \epsilon_2^\top]^\top$, the standard quaternion product is defined as

$$q_1 \otimes q_2 = \begin{bmatrix} \eta_1 & -\epsilon_1^\top \\ \epsilon_1 & \eta_1 I_3 + S(\epsilon_1) \end{bmatrix} \begin{bmatrix} \eta_2 \\ \epsilon_2 \end{bmatrix}.$$

With $\mathbf{1} = [1, 0, 0, 0]^\top \in \mathbf{S}_3$ we denote the identity quaternion element and, for a quaternion $q = [\eta, \epsilon^\top]^\top \in \mathbf{S}_3$, with $q^{-1} = [\eta, -\epsilon^\top]^\top$ the inverse, so that $q \otimes q^{-1} = q^{-1} \otimes q = \mathbf{1}$. A rotation matrix parameterizing attitude can be expressed in terms of a unit quaternion $q \in \mathbf{S}_3$ through the mapping $\mathcal{R} : \mathbf{S}_3 \to SO(3)$ (known as Rodrigues formula [26]) defined as

$$\mathcal{R}(q) = I_3 + 2\eta S(\epsilon) + 2S(\epsilon)^2.$$

The mapping $\mathcal{R}$ is such that $\mathcal{R}(q) = \mathcal{R}(-q)$, namely the two quaternions q and $-q$ correspond to the same rotation matrix.

We refer to a *saturation function* as a mapping $\sigma : \mathbb{R}^n \to \mathbb{R}^n$ such that, for $n = 1$,

1) $|\sigma'(s)| := |d\sigma(s)/ds| \leq 2$ for all s,
2) $|\sigma''(s)| := |d^2\sigma(s)/ds^2| \leq \bar{d}$ for some $\bar{d} > 0$, for all s,
3) $s\sigma(s) > 0$ for all $s \neq 0$, $\sigma(0) = 0$,
4) $\sigma(s) = \text{sgn}(s)$ for $|s| \geq 1$,
5) $|s| < |\sigma(s)| < 1$ for $|s| < 1$.

For $n > 1$, the properties listed above are intended to hold componentwise.

B. Hybrid Systems: Definitions and Stability Notions

In this work, we consider hybrid systems $\mathcal{H}$ given by

$$\mathcal{H} \quad \begin{cases} \dot{x} \in F(x, v_c) & x \in C \\ x^+ \in G(x) & x \in D, \end{cases} \tag{1}$$

with state $x \in \mathbb{R}^n$ and input $v_c \in \mathbb{R}^m$ acting only on the flows. The sets $C \subset \mathbb{R}^n$ and $D \subset \mathbb{R}^n$ define the flow and jump sets, respectively, while the set-valued mappings $F : \mathbb{R}^n \times \mathbb{R}^m \rightrightarrows \mathbb{R}^n$ and $G : \mathbb{R}^n \rightrightarrows \mathbb{R}^n$ define the flow map and jump map, respectively. For details about hybrid systems, see [23].

In the special case in which $v_c \equiv 0$, the hybrid systems considered in this paper will satisfy the *hybrid basic conditions* (see [23]), namely

(A1) The sets C and D are closed in $\mathbb{R}^n$.
(A2) The set-valued mapping $(x, 0) \mapsto F(x, 0)$ is outer semicontinuous relative to $\mathbb{R}^n \times \{0\}$ and locally bounded, and for all $x \in C$, $F(x, 0)$ is nonempty and convex.
(A3) The set-valued mapping $x \mapsto G(x)$ is outer semicontinuous relative to $\mathbb{R}^n$ and locally bounded, and for all $x \in D$, $G(x)$ is nonempty.

1) Solutions: Solutions to hybrid systems $\mathcal{H}$ are given by pairs of *hybrid arcs* and *hybrid inputs* defined over extended time domains called *hybrid time domains*. A set $S \subset \mathbb{R}_{\geq0} \times \mathbb{N}$ is a hybrid time domain if, for all $(T, J) \in S$, the set $S \cap ([0, T] \times \{0, 1, ..., J\})$ can be written as

$$\bigcup_{j=0}^{J-1} ([t_j, t_{j+1}], j)$$

for some finite sequence of times $0 = t_0 \leq t_1 \leq t_2 ... \leq t_J$. A hybrid arc $x : \text{dom}\, x \to \mathbb{R}^n$ is such that $\text{dom}\, x$ is a hybrid time domain and, for each j, $t \mapsto x(t, j)$ is absolutely continuous on the interval $\{t : (t, j) \in \text{dom}\, x\}$. A hybrid arc is parameterized by (t, j), where t is the ordinary-time component and j is the discrete-time component that keeps track of the number of jumps. A hybrid input $v_c : \text{dom}\, v_c \to \mathbb{R}^m$ is such that $\text{dom}\, v_c$ is a hybrid time domain and, for each $j \in \mathbb{N}$, the function

$t \mapsto v_c(t,j)$ is Lebesgue measurable and locally essentially bounded on the interval $\{t \,:\, (t,j) \in \operatorname{dom} v_c\}$. Then, given a hybrid input $v_c : \operatorname{dom} v_c \to \mathbb{R}^m$ and an initial condition ξ, a hybrid arc $\phi : \operatorname{dom}\phi \to \mathbb{R}^n$ defines a *solution pair* (ϕ, v_c) *to the hybrid system* $\mathcal{H}$ in (1) if the following conditions hold:

(S0) $\xi \in \overline{C} \cup D$ and $\operatorname{dom}\phi = \operatorname{dom} v_c \,(= \operatorname{dom}(\phi, v_c))$;

(S1) For each $j \in \mathbb{N}$ such that $I_j := \{t \,:\, (t,j) \in \operatorname{dom}(\phi, v_c)\}$ has nonempty interior $\operatorname{int}(I_j)$, $\phi(t,j) \in C$ for all $t \in \operatorname{int}(I_j)$, and, for almost all $t \in I_j$, $\frac{d}{dt}\phi(t,j) \in F(\phi(t,j), v_c(t,j))$;

(S2) For each $(t,j) \in \operatorname{dom}(\phi, v_c)$ such that $(t, j+1) \in \operatorname{dom}(\phi, v_c)$, $\phi(t,j) \in D$ and $\phi(t, j+1) \in G(\phi(t,j))$.

A solution pair (ϕ, v_c) to $\mathcal{H}$ is said to be *complete* if $\operatorname{dom}(\phi, v_c)$ is unbounded, *maximal* if there does not exist another pair $(\phi, v_c)'$ such that (ϕ, v_c) is a truncation of $(\phi, v_c)'$ to some proper subset of $\operatorname{dom}(\phi, v_c)'$.

2) Stability Notions: For a hybrid system $\mathcal{H}$ with $v_c \equiv 0$, which will be denoted as $\mathcal{H}_0$, the following definition of stability will be used.

Definition 1 *A compact set $\mathcal{A} \subset \mathbb{R}^n$ is said to be*

- stable *if for each $\epsilon > 0$ there exists $\delta > 0$ such that each maximal solution ϕ to $\mathcal{H}_0$ with $|\phi(0,0)|_{\mathcal{A}} \le \delta$ satisfies $|\phi(t,j)|_{\mathcal{A}} \le \epsilon$ for all $(t,j) \in \operatorname{dom}\phi$;*
- attractive *if there exists $\mu > 0$ such that every maximal solution ϕ to $\mathcal{H}_0$ with $|\phi(0,0)|_{\mathcal{A}} \le \mu$ is complete and satisfies*

$$\lim_{(t,j)\in\operatorname{dom}\phi, t+j\to\infty} |\phi(t,j)|_{\mathcal{A}} = 0;$$

- asymptotically stable *if it is stable and attractive*.

Asymptotic stability is said to be global when the attractivity property holds for every point in $\overline{C} \cup D$.

III. Problem Formulation

A. Dynamical Model

The dynamics of a large class of miniature Vertical Take-Off and Landing (VTOL) aerial vehicles, including helicopters, ducted-fan and multi-propeller configurations, can be described by considering the following dynamic model (see among others [21], [15])

$$\begin{aligned} M\ddot{p} &= -u_f R e_3 + M g e_3 + d_f \\ \dot{R} &= RS(\omega) \\ J\dot{\omega} &= S(J\omega)\omega + u_\tau + d_\tau \end{aligned} \tag{2}$$

in which $p = [x,\, y,\, z]^\top \in \mathbb{R}^3$ denotes the position of the center of gravity of the system expressed in the inertial reference frame $\mathcal{F}_i$, $\omega = [\omega_x,\, \omega_y,\, \omega_z]^\top \in \mathbb{R}^3$ is the angular speed expressed in the body frame $\mathcal{F}_b$, $R \in SO(3)$ is the rotation matrix relating vectors in $\mathcal{F}_b$ to vectors in $\mathcal{F}_i$, $M \in \mathbb{R}_>$ and $J \in \mathbb{R}^{3\times 3}$ (with the property that $J = J^\top > 0$) are the mass and the inertia matrix of the system, $u_f \in \mathbb{R}_{\ge 0}$ denotes the control force that, by construction, is directed along the body z axis and $u_\tau \in \mathbb{R}^3$ is the control torque vector. The force and torque vectors $d_f \in \mathbb{R}^3$ and $d_\tau \in \mathbb{R}^3$ are bounded unknown exogenous signals modeling the effects of aerodynamic drag and wind disturbances.

To model actuator limitations, the control force and torques are required to satisfy

$$u_f \in \Omega_f, \quad u_\tau \in \Omega_\tau \tag{3}$$

where the compact sets $\Omega_f \subset \mathbb{R}_{\ge 0}$ and $\Omega_\tau \subset \mathbb{R}^3$ define the attainable force and torques for the specific vehicle.

Besides the presence of the exogenous disturbances d_f and d_τ, the further source of uncertainty considered in the paper is the inertia matrix J. More specifically, it is assumed that only a nominal value $J_0 \in \mathbb{R}^{3\times 3}$, with $J_0 = J_0^\top > 0$, and an "upper-bound" $J^U \in \mathbb{R}^{3\times 3}$, i.e., such that

$$|x^\top J^U x| \ge |x^\top J x| \tag{4}$$

for all $x \in \mathbb{R}^3$, are known. This uncertainty on the value of J reflects the fact that, for a physical system having a complex mass distribution, an exact inertia matrix may not be available.

Remark 1 *Instead of using a rotation matrix R, the attitude in (2) can be parameterized by means of the unit quaternion $q \in \mathbf{S}_3$. In this case, in the first equation in (2) the rotation matrix is replaced by the Rodrigues map $\mathcal{R}$ and the kinematic equations, which are given by the second equation in (2), are replaced by*

$$\dot{q} = \frac{1}{2} q \otimes \begin{bmatrix} 0 \\ \omega \end{bmatrix}. \tag{5}$$

In many applications, quaternion parametrization of attitude is often preferred due to the small number of parameters (4 with respect to 9 required by a rotation matrix) and the computationally simple quaternion algebra [26].

B. Control Problem and Nominal System Inversion

This work focuses on the problem of *global* tracking by state feedback for system (2). More specifically, the goal is to asymptotically track a given time reference position and orientation

$$t \mapsto p^*(t) \in \mathbb{R}^3, \quad t \mapsto R^*(t) \in SO(3) \tag{6}$$

for all possible initial conditions $p(0) \in \mathbb{R}^3$, $\dot{p}(0) \in \mathbb{R}^3$, $R(0) \in SO(3)$, $\omega(0) \in \mathbb{R}^3$, by assuming full knowledge of the state of the system.

Two different scenarios will be considered. The first scenario, referred to as the *nominal case*, is when the force and the torque disturbances are neglected, i.e., $d_f \equiv d_\tau \equiv 0$, and the inertia matrix is perfectly known, i.e., $J^U \equiv J_0 \equiv J$. The second scenario, referred to as the *robust case*, takes into account all of the uncertainties specified in Section III-A. Due to the presence of disturbances, a *practical* tracking result will be derived in the *robust case*, while *asymptotic* tracking results are obtained in the *nominal case*.

The desired references (6) are required to satisfy *functional controllability* constraints that are described below. The first constraint derives from the under-actuated nature of system (2) by which the reference position and orientation cannot

be assigned independently. As the aircraft position assumes a major role in real-world applications [1], the attitude reference is required to satisfy some constraints to meet the requirements posed by the position tracking objective. Specifically, let $t \mapsto p^*(t)$ be the desired position reference and let $t \mapsto v_f^*(t)$ be the *nominal reference control force vector* defined as

$$v_f^*(t) := Mge_3 - M\ddot{p}^*(t) \quad \forall t \geq 0\,. \tag{7}$$

The function in (7) represents the force vector yielding the desired acceleration $\ddot{p}^*(t)$ in the *nominal case* (i.e., when $d_f \equiv 0$). The enforcement of such a $v_f^*(t)$ necessarily requires that the body z-axis of the vehicle, i.e., the thrust direction, is aligned with $v_f^*(t)$ at each t. This requires that the reference attitude $t \mapsto R^*(t) \in SO(3)$ satisfies the following constraint

$$R^*(t)e_3 = \frac{v_f^*(t)}{|v_f^*(t)|} \quad \forall t \geq 0\,. \tag{8}$$

Implicit in the previous expression is the requirement that $t \mapsto \ddot{p}^*(t)$ is such that

$$|v_f^*(t)| = M|ge_3 - \ddot{p}^*(t)| > \underline{v}, \ \forall t \geq 0 \tag{9}$$

for some $\underline{v} \in \mathbb{R}_{>0}$, which is assumed hereafter.

The problem of computing a rotation matrix satisfying (8) has been considered, for instance, in [16] using differential geometric tools, and in [15] using a unit quaternion parametrization of R^*. Details on the computation of a rotation matrix R^* fulfilling (8) are presented in Appendix C.

With $t \mapsto v_f^*(t)$ and $t \mapsto R^*(t)$ fulfilling (8) and (9) in hand, the nominal system inversion can be accomplished by defining the reference force and torque control inputs as

$$u_f^*(t) \quad := \quad |v_f^*(t)| \tag{10}$$

and

$$u_\tau^*(t) \quad := \quad J\dot{\omega}^*(t) - S(J\omega^*(t))\omega^*(t)\,,$$

for each $t \geq 0$, where $\omega^*(t) := (R^{*T}(t)\dot{R}^*(t))^\wedge$ is the reference angular velocity. Note that u_τ^* depends on the uncertain parameter J; hence, it can be computed only in the *nominal case*. In the following, for the sake of clarity, we shall denote by $u_{\tau 0}^*$ the nominal value of u_τ^*, namely

$$u_{\tau 0}^* \quad := \quad J_0\dot{\omega}^* - S(J_0\omega^*)\omega^*\,. \tag{11}$$

The reference angular velocity ω^* and its time derivative along the body x and y axis can be easily derived as functions of p^* and its time derivatives. As a matter of fact, using the second equation in (2), it follows that $R^{*\top}\dot{R}^*e_3 = S(\omega^*)e_3$ by which

$$\begin{bmatrix} \omega_x^* \\ \omega_y^* \end{bmatrix} := W_{xy}R^{*\top}\frac{d}{dt}\frac{v_f^*}{|v_f^*|}\,, \tag{12}$$

$$\begin{bmatrix} \dot{\omega}_x^* \\ \dot{\omega}_y^* \end{bmatrix} := W_{xy}\left(-S(\omega^*)R^{*\top}\frac{d}{dt}\frac{v_f^*}{|v_f^*|} + R^{*\top}\frac{d^2}{dt^2}\frac{v_f^*}{|v_f^*|}\right)$$

where $W_{xy} \in \mathbb{R}^{2\times 3}$ is the matrix with the first and second rows given by $[0, -1, 0]$ and $[1, 0, 0]$, respectively. On the other hand, the angular speed and acceleration along the body z-axis, namely $t \mapsto \omega_z^*$ and $\dot{\omega}_z^*$, are not subjected to constraints deriving from the position tracking objective.

Further constraints on the reference position $t \mapsto p^*(t)$ and the reference orientation $t \mapsto R^*(t)$ must be chosen to let the control force and torques computed in (10) and (11) satisfy the actuator limitations (3), namely

$$u_f^*(t) \in \Omega_f, \ \ u_\tau^*(t) \in \Omega_\tau \ \ \forall t \geq 0\,. \tag{13}$$

In particular, the reference derivatives $p^{*\,(1)}$, $p^{*\,(2)}$, $p^{*\,(3)}$, $p^{*\,(4)}$, ω_z^* and $\omega_z^{*\,(1)}$ are required to be bounded functions of time satisfying appropriate bounds.

Remark 2 *Let $R_1 \in SO(3)$ be such that (8) holds with $R^* = R_1$. Then (8) also holds by picking $R^* = R_1R_z$ for any $R_z \in SO(3)$ such that $R_ze_3 = e_3$ (i.e., R_z represents an elementary rotation around the e_3 unit vector). This fact shows that the relation given in (8) fixes only two of the three degree of freedom of R^*. The third degree of freedom, which is the rotation around the vector $v_f^*(t)$, can be arbitrarily assigned according to attitude tracking objectives.*

IV. Inner-Outer Loop Control Strategies

This section presents control strategies that solve the global tracking problem in the *nominal* and *robust* case. The proposed solutions rely upon a hierarchical control structure having the attitude and the position closed-loop dynamics playing the role of the *inner loop* and of the *outer loop*, respectively. A *vectored-thrust* control paradigm (see [21]) is followed in the design of the control law. In this respect, a crucial role in avoiding singularities is played by the use of saturation functions in the outer loop that naturally lead to the design of a "control vectored-thrust" whose amplitude never vanishes regardless of the values assumed by the position error. This feature, in turn, enables the adoption of vectored-thrust design paradigms in setting up references signal for the attitude dynamics on which the inner loop is built.

As far as the inner loop is concerned, two different control strategies are presented to address the *nominal* and *robust cases*, respectively. In the *nominal case*, the torque control input is synthesized as a "feedback linearizing" control law able to decouple the closed-loop attitude dynamics from the position dynamics. The resulting control loop, which is depicted Figure 1(a), is a *cascade* interconnection between the attitude and the position loops. In the next subsections, it is shown that stability of the overall interconnected system does not impose constraints on the tuning of the position and attitude controllers. The above property can be also achieved by designing a torque control input able to only partially decouple the closed-loop attitude and position dynamics. This leads to the feedback interconnection depicted in Figure 1(b), in which, due to a suitable design of the torque control input, the influence of the position dynamics on the attitude dynamics does not affect the stability properties of the overall closed-loop system.

In the *robust case*, a complete decoupling of the closed-loop attitude and position dynamics is not possible. In this case, the proposed attitude controller combines only a linear feedback law, driven by a hybrid system to overcome the topological obstruction, and a feed-forward law obtained by

model inversion This control law will lead to a feedback interconnection between the attitude (inner) and the position (outer) loop (see Figure 1(c)). In the stability analysis of this feedback interconnection, a crucial role is played by the use of nested saturation functions (used in the outer loop) introducing a "decoupling effect" between the two interconnected dynamics. Such an effect, in turn, is crucial to show that the attitude loop, which is a hybrid system, has solutions that, after some finite time, only flow. This property of solutions is instrumental to establish asymptotic properties of the feedback interconnection.

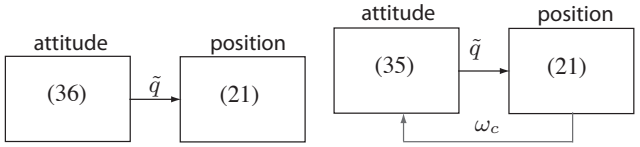

(a) Nominal Case: Cascade Interconnection

(b) Nominal Case: Feedback Interconnection

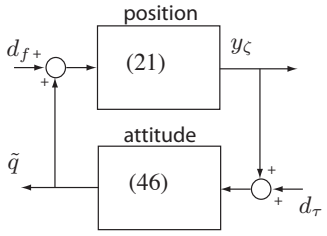

(c) Robust Case: Feedback Interconnection

Fig. 1. The resulting inner/outer loops in the nominal and robust cases.

A. Stabilization of the translational motion

By letting

$$\tilde{\mathbf{p}} := \begin{bmatrix} \tilde{p} \\ \dot{\tilde{p}} \end{bmatrix} := \begin{bmatrix} p - p^* \\ \dot{p} - \dot{p}^* \end{bmatrix}$$

and bearing in mind the first equation in (2), the position error dynamics are described by

$$M\ddot{\tilde{p}} = -u_f R e_3 + v_f^* + d_f \tag{14}$$

with v_f^* defined in (7). A vectored-thrust control strategy is employed to stabilize system (14). To this end, let the *control force vector* v_c be defined as

$$v_c(\tilde{\mathbf{p}}, t) := v_f^*(t) + \kappa(\tilde{\mathbf{p}}), \tag{15}$$

where κ is a state feedback law satisfying $\kappa(0) = 0$ and

$$|\kappa(\tilde{\mathbf{p}})| \leq \bar{\kappa} \qquad \forall\, \tilde{\mathbf{p}} \in \mathbb{R}^6 \tag{16}$$

with $0 < \bar{\kappa} < \underline{v}$. Property (16), which will be fulfilled in the following by designing $\kappa(\cdot)$ as a saturated function, guarantees that

$$|v_c(\tilde{\mathbf{p}}, t)| \geq |v_f^*(t)| - |\kappa(\tilde{\mathbf{p}})| \geq \underline{v} - \bar{\kappa} > 0 \tag{17}$$

for all $\tilde{\mathbf{p}} \in \mathbb{R}^6$ and $t \geq 0$. The form of (14) suggests to design the force control input $u_f \in \mathbb{R}_{>0}$ and a desired reference attitude $R_c \in SO(3)$ in such a way that $u_f(t) R_c(\tilde{\mathbf{p}}, t) e_3 = v_c(\tilde{\mathbf{p}}, t)$, namely

$$R_c(\tilde{\mathbf{p}}, t) e_3 \quad = \quad \frac{v_c(\tilde{\mathbf{p}}, t)}{|v_c(\tilde{\mathbf{p}}, t)|} \tag{18}$$

and

$$u_f = u_{fc}(\tilde{\mathbf{p}}, t) := |v_c(\tilde{\mathbf{p}}, t)|\,. \tag{19}$$

Note that (18), (19) are well defined for all $\tilde{\mathbf{p}} \in \mathbb{R}^6$ and for all $t \geq 0$ by virtue of (17) and of (16). By bearing in mind the discussion in Remark 2, relation (18) fixes two of the three degree of freedom characterizing $R_c \in SO(3)$. The third degree of freedom can be fixed by enforcing the constraint

$$R_c(0, t) = R^*(t) \quad \forall t \geq 0 \tag{20}$$

which, along with (18), uniquely defines the control reference attitude $R_c \in SO(3)$.

By adding and subtracting the term $u_f R_c e_3$ in (14), the position error dynamics read as

$$M\ddot{\tilde{p}} = -\kappa(\tilde{\mathbf{p}}) + \Gamma(R_c, R) + d_f \tag{21}$$

where Γ is defined as

$$\Gamma(R_c, R) := u_{f_c} (R_c - R)\, e_3\,. \tag{22}$$

The design of $\kappa(\cdot)$ must be conceived to stabilize the origin of (21), which is a double integrator forced by the exogenous inputs Γ and d_f, and to fulfill the crucial requirement (16). Nested saturations can be used for such a purpose ([27], [20]). Among the possible nested saturation design solutions available in literature (see, for instance, [27], [28], [29]), the approach in [20, Appendix C] yields the following control law

$$\kappa(\tilde{\mathbf{p}}) := \lambda_2 \sigma \left(\frac{k_2}{\lambda_2} \left(\dot{\tilde{p}} + \lambda_1 \sigma \left(\frac{k_1}{\lambda_1} \tilde{p} \right) \right) \right) \tag{23}$$

in which σ is a saturation function defined in Section II while λ_1, λ_2, k_1, and k_2 are chosen as

$$\lambda_i = \varepsilon^{(i-1)}\, \lambda_i^\star, \qquad k_i = \varepsilon\, k_i^\star, \qquad i = 1, 2 \tag{24}$$

where $k_i^\star$, $\lambda_i^\star$ are positive constants (fixed as Proposition 1 below) and $\varepsilon > 0$. Note that, by the definition of saturation function,

$$|\kappa(\tilde{\mathbf{p}})| \leq \sqrt{3}\, \lambda_2^\star \varepsilon\,.$$

Property (16) is thus fulfilled by fixing ε as

$$0 < \varepsilon \leq \frac{\bar{\kappa}}{\sqrt{3} \lambda_2^\star}\,. \tag{25}$$

The asymptotic properties of the closed-loop position system (21), (23) are detailed in the following proposition.

Proposition 1 *Consider the closed-loop position error dynamics (21)-(23) with λ_i and k_i, $i = 1, 2$, chosen as in (24), (25) and $\lambda_i^\star$, $k_i^\star$ taken as*

$$\frac{\lambda_2^\star}{k_2^\star} < \frac{\lambda_1^\star}{4}, \qquad 4 k_1^\star \lambda_1^\star < \frac{\lambda_2^\star}{4}, \qquad 6 \frac{k_1^\star}{k_2^\star} < \frac{1}{24}\,. \tag{26}$$

Then, there exist $R_\Gamma > 0$, $R_{d_f} > 0$ and $\gamma_{\text{pos}} > 0$ such that the system is Input-to-State Stable with respect to the inputs (Γ, d_f) without restrictions on the initial state, restrictions

$(R_\Gamma,\ R_{d_f})$ on the inputs and asymptotic gain $\gamma_{\rm pos}$. In particular, for all (Γ, d_f) such that $|\Gamma|_\infty \leq R_\Gamma$, $|d_f|_\infty \leq R_{d_f}$ and for all initial conditions $\tilde{\mathbf{p}}(0) \in \mathbb{R}^6$, the resulting trajectories are bounded and the following asymptotic bound holds true

$$|\tilde{\mathbf{p}}|_a \leq \gamma_{\rm pos}\ \max\{\,|\Gamma|_a\,,\ |d_f|_a\,\}\,.$$

Proof: System (21)-(23) can be rewritten as

$$\begin{aligned}\dot{\zeta}_1 &= -\lambda_1\sigma\left(\tfrac{k_1}{\lambda_1}\zeta_1\right)+\zeta_2\\ M\dot{\zeta}_2 &= -\lambda_2\sigma\left(\tfrac{k_2}{\lambda_2}\zeta_2\right)+Mk_1\sigma'\left(\tfrac{k_1}{\lambda_1}\zeta_1\right)\dot{\zeta}_1+\gamma(R_c,R)+\\ &+\ d_f\end{aligned}$$

where $\zeta_1 := \tilde{p}$, $\zeta_2 := \dot{\tilde{p}} + \lambda_1\sigma\left((k_1/\lambda_1)\zeta_1\right)$. Then the result follows from [20, Lemma C.2.1] and [20, Proposition C.2.2] since the system can be written as [20, (C.7)] with $n = 2$, $q_1 = 1$, $q_2 = 1/M$, $v_1 = 0$ and $v_2 = (\Gamma(\cdot) + d_f)/M$. □

If $R = R_c$ then $\Gamma \equiv 0$ and the previous result shows that the position tracking error has an asymptotic bound upper bounded by a function of the disturbance d_f. Due to the fact that saturation functions are used in the design of $\kappa(\cdot)$, the class of force disturbances is required to fulfill the restriction $|d_f|_\infty \leq R_{d_f}$. In particular, if $d_f \equiv 0$, global asymptotic tracking is guaranteed. In the next subsection, we show how the attitude dynamics of the vehicle can be controlled in order to asymptotically enforce the condition $R = R_c$. This is accomplished through appropriate design of the inner loop, in which the rotation matrix R_c plays the role of reference signal for the attitude dynamics.

Instrumental to the design of the inner loop is the computation of the angular velocity ω_c associated to the rotation matrix R_c, defined as

$$\omega_c = (R_c^\top \dot{R}_c)^\wedge\,.$$

The next two lemmas exploit the particular choice of the position control law (23) to highlight some properties of ω_c and $\dot{\omega}_c$ that will play a key role in the subsequent analysis.

Lemma 1 *The angular velocity ω_c can be expressed as*

$$\omega_c = \Omega_1(\tilde{\mathbf{p}},t) + \Omega_2(\tilde{\mathbf{p}},t)\,\Gamma(R,R_c) + \Omega_2(\tilde{\mathbf{p}},t)\,d_f$$

where Ω_1 and Ω_2 are smooth functions satisfying $\Omega_1(0,t) = \omega^\star(t)$ for all $t \geq 0$ and

$$|\Omega_i(\tilde{\mathbf{p}},t)| \leq \bar{\Omega} \qquad \forall\ \tilde{\mathbf{p}} \in \mathbb{R}^6\,,\ t \geq 0$$

$i \in \{1,\,2\}$, with $\bar{\Omega}$ a positive constant.

Proof: See Appendix A. □

Lemma 2 *If $d_f \equiv 0$ then there exist $\bar{\Omega}_{c1}, \bar{\Omega}_{c2} \in \mathbb{R}_{\geq 0}$ such that*

$$|\omega_c|_\infty \leq \bar{\Omega}_{c1} \text{ and } |\dot{\omega}_c|_\infty \leq \bar{\Omega}_{c2}\,.$$

Proof: See Appendix B. □

The next two subsections present the attitude stabilization in the nominal and robust case, respectively. The analysis in those sections is based on a quaternion parametrization of the attitude. In this respect, we denote by $q_c \in \mathbf{S}_3$ a *control quaternion* associated to R_c, namely $\mathcal{R}(q_c) = R_c$ with $\mathcal{R}(\cdot)$ the Rodrigues map. Due to topological reasons, the computation of q_c from R_c requires lifting continuous paths from $SO(3)$ to $\mathbf{S}_3$. In this paper, this has been achieved by employing the path-lifting mechanism proposed in [30], which ensures that $t \mapsto q_c(t)$ is a continuous function of time.

B. Attitude Stabilization: the Nominal Case

Let us consider the problem of attitude stabilization in the *nominal case* in which $d_f \equiv 0$, $d_\tau \equiv 0$, and $J \equiv J_0$. We start by defining attitude error coordinates as

$$\begin{aligned}\tilde{q} &:= q_c^{-1} \otimes q\\ \tilde{\omega}_c &:= \omega - \bar{\omega}_c\end{aligned} \tag{27}$$

with $\bar{\omega}_c := R(\tilde{q})^\top \omega_c$. From (27), bearing in mind (5) and the last equation in (2), the following error attitude dynamics can be computed

$$\begin{aligned}\dot{\tilde{q}} &= \frac{1}{2}\tilde{q} \otimes \begin{bmatrix} 0 \\ \tilde{\omega}_c \end{bmatrix}\\ J\dot{\tilde{\omega}}_c &= \Sigma(\tilde{\omega}_c,\bar{\omega}_c)\tilde{\omega}_c + S(J\bar{\omega}_c)\bar{\omega}_c - J\mathcal{R}(\tilde{q})^\top\dot{\omega}_c + u_\tau\,,\end{aligned} \tag{28}$$

having defined by Σ the skew-symmetric matrix

$$\Sigma(\tilde{\omega}_c,\bar{\omega}_c) := S(J\tilde{\omega}_c) + S(J\bar{\omega}_c) - S(\bar{\omega}_c)J - JS(\bar{\omega}_c)\,.$$

Hereafter, the scalar and vector part of the error quaternion $\tilde{q}$ are denoted, respectively, by $\tilde{\eta}$ and $\tilde{\epsilon}$.

Inspired by [22], the following two controllers are designed

$$u_\tau = u_{\tau,FF}(\tilde{q},\omega_c,\dot{\omega}_c) + u_{\tau,FB}(\tilde{q},\tilde{\omega}_c,h)\,, \tag{29}$$

$$u'_\tau = u'_{\tau,FF}(\tilde{q},\omega_c,\dot{\omega}_c) + u_{\tau,FB}(\tilde{q},\tilde{\omega}_c,h) \tag{30}$$

where $u_{\tau,FF}(\cdot)$ and $u'_{\tau,FF}(\cdot)$ are the "feedforward terms", which are given by

$$u_{\tau,FF}(\tilde{q},\omega_c,\dot{\omega}_c) = J\mathcal{R}(\tilde{q})^\top\dot{\omega}_c - S(J\bar{\omega}_c)\bar{\omega}_c \tag{31}$$

and

$$u'_{\tau,FF}(\tilde{q},\omega_c,\dot{\omega}_c) = u_{\tau,FF} - \left(\Sigma(\tilde{\omega}_c,\,\bar{\omega}_c) - S(J\tilde{\omega}_c)\right)\tilde{\omega}_c\,, \tag{32}$$

while $u_{\tau,FB}$ is the "hybrid feedback term"

$$u_{\tau,FB}(\tilde{q},\tilde{\omega}_c,h) = -k_p\,h\,\tilde{\epsilon} - k_d\,\tilde{\omega}_c \tag{33}$$

in which k_p, k_d are positive gains and where $h \in \{-1,\,1\}$ is a logic variable with hysteresis governed by the hybrid dynamics

$$\begin{cases} \dot{h} = 0 & h\,\tilde{\eta} \geq -\delta \\ h^+ \in \overline{\rm sgn}(\tilde{\eta}) & h\,\tilde{\eta} \leq -\delta \end{cases} \tag{34}$$

where $\delta \in (0,\,1)$ is the hysteresis threshold and $\overline{\rm sgn} : \mathbb{R} \rightrightarrows \{-1,1\}$ is the set-valued function

$$\overline{\rm sgn}(s) = \begin{cases} {\rm sgn}(s) & |s| > 0 \\ \{-1,1\} & s = 0\,. \end{cases}$$

The goal of the control law (30) is to completely decouple the attitude from the position dynamics in order to obtain the cascade connection given in Figure 1(a). The control law (29), on the other hand, is such that the skew-symmetric

term $\Sigma(\tilde{\omega}_c, \bar{\omega}_c)\tilde{\omega}_c$ in (28) is not canceled, leading to the interconnection shown in Figure 1(b).

By considering the control torques (29) and (30), the corresponding closed-loop attitude error systems, denoted respectively as $\mathcal{H}_{\rm nom}$ and $\mathcal{H}'_{\rm nom}$, are given by

$$\mathcal{H}_{\rm nom} \left\{ \begin{array}{ll} \dot{\tilde{x}} = F_{\rm nom}(\tilde{x}, \omega_c) & \tilde{x} \in C_{\rm nom} \\ \tilde{x}^+ \in G_{\rm nom}(\tilde{x}) & \tilde{x} \in D_{\rm nom} \end{array} \right. \tag{35}$$

and

$$\mathcal{H}'_{\rm nom} \left\{ \begin{array}{ll} \dot{\tilde{x}} = F'_{\rm nom}(\tilde{x}) & \tilde{x} \in C_{\rm nom} \\ \tilde{x}^+ \in G_{\rm nom}(\tilde{x}) & \tilde{x} \in D_{\rm nom} \end{array} \right. \tag{36}$$

where $\tilde{x} = {\rm col}(\tilde{q},\, \tilde{\omega}_c,\, h)$,

$$F_{\rm nom}(\tilde{x}, \omega_c) := \left[\begin{array}{c} \frac{1}{2}\tilde{q} \otimes \left[\begin{array}{c} 0 \\ \tilde{\omega}_c \end{array} \right] \\ J^{-1}\left(\Sigma(\tilde{\omega}_c, \bar{\omega}_c)\, \tilde{\omega}_c - k_p\, h\, \tilde{\epsilon} - k_d\, \tilde{\omega}_c \right) \\ 0 \end{array} \right],$$

$$F'_{\rm nom}(\tilde{x}) := \left[\begin{array}{c} \frac{1}{2}\tilde{q} \otimes \left[\begin{array}{c} 0 \\ \tilde{\omega}_c \end{array} \right] \\ J^{-1}\left(S(J\tilde{\omega}_c)\tilde{\omega}_c - k_p\, h\, \tilde{\epsilon} - k_d\, \tilde{\omega}_c \right) \\ 0 \end{array} \right],$$

$$G_{\rm nom}(\tilde{x}) := [\tilde{q}^\top,\, \tilde{\omega}_c^\top,\, \overline{\rm sgn}(\tilde{\eta})]^\top,$$

$$C_{\rm nom} := \{\tilde{x} \in \mathcal{X}_{att} \,:\, h\,\tilde{\eta} \geq -\delta\},$$

$$D_{\rm nom} := \{\tilde{x} \in \mathcal{X}_{att} \,:\, h\,\tilde{\eta} \leq -\delta\}$$

having defined $\mathcal{X}_{att} := \mathbf{S}_3 \times \mathbb{R}^3 \times \{-1, 1\}$. Note that the attitude error system (35) is affected by the position error system through the input ω_c, whereas the attitude error system (36), as a consequence of the choice (32), is an autonomous system. Also note that $F_{\rm nom}(0, \omega_c) = 0$ for all $\omega_c \in \mathbb{R}^3$.

For the closed-loop autonomous system (36), inspired by the ideas in [22], we have the following result.

Proposition 2 *Consider the hybrid systems $\mathcal{H}'_{\rm nom}$ in (36). For all $k_p > 0$, $k_d > 0$, and $\delta \in (0,\, 1)$, the compact set*

$$\mathcal{A} = \{\tilde{x} \in \mathcal{X}_{att} \,:\, \tilde{q} = h\mathbf{1}\,,\, \tilde{\omega}_c = 0\}$$

is globally asymptotically stable.

Proof: Consider the candidate Lyapunov function $V : \mathcal{X}_{att} \to \mathbb{R}_{\geq 0}$ given by $V(\tilde{x}) = 2k_p(1 - h\tilde{\eta}) + \frac{1}{2}\tilde{\omega}_c^\top J\tilde{\omega}_c$. It satisfies $V(\mathcal{A}) = 0$, $V(\mathcal{X}_{att} \setminus \mathcal{A}) > 0$, and $\{\tilde{x} \in \mathcal{X}_{att} : V(\tilde{x}) \leq c\}$ is compact for every $c \geq 0$. During flows, since

$$\dot{\tilde{\eta}} \;=\; -\frac{1}{2}\,\tilde{\epsilon}^\top\,\tilde{\omega}_c, \quad \dot{\tilde{\epsilon}} \;=\; \frac{1}{2}\tilde{\eta}\,\tilde{\omega}_c + \frac{1}{2}\,S(\tilde{\epsilon})\,\tilde{\omega}_c$$

and $\tilde{\omega}_c^\top S(J\tilde{\omega}_c)\tilde{\omega}_c = 0$ we have

$$\langle \nabla V(\tilde{x}), F'_{\rm nom}(\tilde{x})\rangle = -k_d\,\tilde{\omega}_c^\top\,\tilde{\omega}_c \leq 0$$

for all $\tilde{x} \in C_{\rm nom}$. During jumps, using the fact $\tilde{x} \in D_{\rm nom}$ implies ${\rm sgn}\tilde{\eta} \neq {\rm sgn}h$ and $h^+ = -h$,

$$\begin{array}{rcl} V(\xi) - V(\tilde{x}) & = & -2k_p(-h)\tilde{\eta} + 2k_p h\tilde{\eta} = 4k_p h\tilde{\eta} \\ & \leq & -4k_p\delta < 0 \end{array}$$

for all $\xi \in G_{\rm nom}(\tilde{x})$ and for all $\tilde{x} \in D_{\rm nom}$. Stability of $\mathcal{A}$ follows by applying [31, Theorem 7.6]. To prove asymptotic stability we make use of an invariance principle. Note first of all that system (36) satisfies assumptions (A1)-(A3). In fact, $C_{\rm nom}$ and $D_{\rm nom}$ are closed sets. The flow map is continuous while, since $s \mapsto \overline{sgn}(s)$ is an outer-semicontinuous and bounded map, $\bar{G}_{\rm nom}$ is outer semi-continuous and locally bounded. Now applying [31, Theorem 4.7] with $u_c : C_{\rm nom} \to \mathbb{R}$ given by $u_c(\tilde{x}) = -k_d\,\tilde{\omega}_c^\top\,\tilde{\omega}_c$ and $u_d : D_{\rm nom} \to \mathbb{R}$ given by $u_d(\tilde{x}) = -4k_p\delta < 0$, it follows that every bounded and complete solution to (36) converges to the largest weakly invariant set contained in

$$V^{-1}(r) \cap W \tag{37}$$

for some $r \geq 0$ where $W := \{\tilde{x} \in C_{\rm nom} \,:\, \tilde{\omega}_c = 0\}$. By evaluating the dynamics (36) along solutions that remain in (37), we have that $\tilde{\epsilon} = 0$ and, since $h\tilde{\eta} \geq -\delta$ for all $\tilde{x} \in W$, $\tilde{q} = h\mathbf{1}$. Then, since the only invariant set is for $r = 0$, i.e., $\{\tilde{x} \in \mathcal{X}_{att} \,:\, \tilde{q} = h\mathbf{1},\, \tilde{\omega}_c = 0,\, h \in \{-1, 1\}\}$, and (37) with $r = 0$ is contained in $\mathcal{A}$, we have that every bounded and complete solution converges to $\mathcal{A}$. Now it remains to prove that every maximal solution is complete and that solutions are bounded. From the fact that $\{\tilde{x} \in \mathcal{X}_{att} : V(\tilde{x}) \leq c\}$ is compact for every $c \geq 0$ and the fact that V is nonincreasing along solutions to (36), we have that solutions are bounded. Moreover, since the viability condition (VC) in [23, Proposition 6.10] holds for (36), $G_{\rm nom}(D_{\rm nom}) \subset (C_{\rm nom} \cup D_{\rm nom})$, and the fact that solutions are bounded, by applying [23, Proposition 6.10], it follows that all maximal solutions are complete. Then $\mathcal{A}$ is attractive. Global asymptotic stability follows from compactness of sublevel sets and from the fact that V is positive definite. □

Now consider system $\mathcal{H}_{\rm nom}$. The latter is a hybrid system affected by the exogenous input ω_c. As a consequence of Lemma 2, we have that the trajectories ω_c can be thought of solutions to the exosystem

$$\dot{\omega}_{\rm e} \;\in\; \mathcal{B}^3_{\bar{\Omega}_{c2}}, \quad \omega_{\rm e} \in \mathcal{B}^3_{\bar{\Omega}_{c1}} \tag{38}$$

in which $\bar{\Omega}_{c1}$, $\bar{\Omega}_{c2}$ are the positive values given in Lemma 2. In particular, we have that there exists a solution $\omega_{\rm e}$ to (38) such that $\omega_{\rm e}(t) \equiv \omega_c(t)$ for all $t \geq 0$. Consider now the autonomous hybrid system given by

$$\mathcal{H}_{\rm e} \left\{ \begin{array}{ll} \dot{x}_{\rm e} \in F_{\rm e}(x_{\rm e}) & x_{\rm e} \in C_{\rm e} \\ \dot{x}_{\rm e} \in G_{\rm e}(x_{\rm e}) & x_{\rm e} \in D_{\rm e} \end{array} \right. \tag{39}$$

where $x_{\rm e} := [\omega_{\rm e}^\top,\, \tilde{x}^\top]^\top$,

$$F_{\rm e}(x_{\rm e}) := \left[\begin{array}{c} \mathcal{B}^3_{\bar{\Omega}_{c2}} \\ F_{\rm nom}(\tilde{x}, \omega_{\rm e}) \end{array} \right],\; G_{\rm e}(x_{\rm e}) := \left[\begin{array}{c} \omega_{\rm e} \\ G_{\rm nom}(\tilde{x}) \end{array} \right]$$

$C_{\rm e} := \{x_{\rm e} \,:\, \omega_{\rm e} \in \mathcal{B}^3_{\bar{\Omega}_{c1}},\, \tilde{x} \in C_{\rm nom}\}$ and $D_{\rm e} := \{x_{\rm e} \,:\, \omega_{\rm e} \in \mathcal{B}^3_{\bar{\Omega}_{c1}},\, \tilde{x} \in D_{\rm nom}\}$. For system (39), the following stability result holds.

Proposition 3 *Consider the hybrid system $\mathcal{H}_{\rm e}$ in (39). For all $k_p > 0$, $k_d > 0$, and $\delta \in (0,\, 1)$, the compact set*

$$\mathcal{A} = \left\{x_{\rm e} \in \mathbb{R}^3 \times \mathcal{X}_{att} \,:\, \omega_{\rm e} \in \mathcal{B}^3_{\bar{\Omega}_{c1}}\,,\, \tilde{q} = h\mathbf{1}\,,\, \tilde{\omega}_c = 0\right\}$$

is globally asymptotically stable.

Proof: Similarly to the proof of Proposition 2, we consider the candidate Lyapunov function $V : \mathcal{B}^3_{\bar{\Omega}_{c1}} \times \mathcal{X}_{att} \to \mathbb{R}_{\geq 0}$ given by $V(x_{\rm e}) = 2k_p(1-h\tilde{\eta}) + \frac{1}{2}\tilde{\omega}_c J \tilde{\omega}_c$. It satisfies $V(\mathcal{A}) = 0$ and $V(\{\mathcal{B}^3_{\bar{\Omega}_{c1}} \times \mathcal{X}_{att}\} \setminus \mathcal{A}) > 0$. Moreover, since $\mathcal{B}^3_{\bar{\Omega}_{c1}}$ is compact, $\{x_{\rm e} \in \mathcal{B}^3_{\bar{\Omega}_{c1}} \times \mathcal{X}_{att} : V(x_{\rm e}) \leq c\}$ is compact for every $c \geq 0$.

During flows, since Σ is a skew-symmetric matrix (which implies $\tilde{\omega}_c^\top \Sigma(\tilde{\omega}_c, \omega_{\rm e})\tilde{\omega}_c = 0$), it turns out that the Lyapunov function is nonincreasing, i.e.,

$$\langle \nabla V(x_{\rm e}), F_{\rm e}(x_{\rm e}) \rangle = -k_d\, \tilde{\omega}_c^\top\, \tilde{\omega}_c \leq 0$$

for all $x_{\rm e} \in C_{\rm e}$. During jumps, following the same arguments as in the proof of Proposition 2,

$$\begin{aligned} V(\xi) - V(x_{\rm e}) &= -2k_p h^+ \tilde{\eta} + 2k_p h \tilde{\eta} = 4k_p h \tilde{\eta} \\ &\leq -4k_p \delta < 0 \end{aligned}$$

for all $\xi \in G_{\rm e}(x_{\rm e})$ and for all $x_{\rm e} \in D_{\rm e}$. Stability of $\mathcal{A}$ follows from [31, Theorem 7.6]. Asymptotic stability can be proved by applying an invariance principle as for the proof of Proposition 2. Note first of all that system (39) satisfies assumptions (A1)-(A3). In fact $C_{\rm e}$ and $D_{\rm e}$ are closed sets. The flow equation is continuous while $\bar{G}_{\rm e}$ is outer semi-continuous and locally bounded. Now applying [31, Theorem 4.7] with $u_c : C_{\rm e} \to \mathbb{R}$ given by $u_c(x_{\rm e}) = -k_d\, \tilde{\omega}_c^\top\, \tilde{\omega}_c$ and $u_d : D_{\rm e} \to \mathbb{R}$ given by $u_d(x_{\rm e}) = -4k_p\delta < 0$, it follows that every bounded and complete solution to (39) converges to the largest weakly invariant set contained in $V^{-1}(r) \cap W$ with $W := \{x_{\rm e} \in C_{\rm e} : \tilde{\omega}_c = 0\}$ and for some $r \geq 0$. Following the same arguments as in the proof of Proposition 2, this implies that every bounded and complete solution converges to $\mathcal{A}$. Global asymptotic stability of $\mathcal{A}$ then follows as in the proof of Proposition 2. □

C. Stability Properties of the Combined Position and Attitude Closed-Loops in the Nominal Case

By combining the ISS properties of the position error system in Proposition 1 with the global asymptotic stability of the attitude error subsystem given in Propositions 2 and 3, the desired global tracking objective for the whole system in the *nominal case* can be accomplished.

Proposition 4 *Consider the closed-loop system given by the position error dynamics (21), with $d_f \equiv 0$, controlled by (23), with λ_i and k_i, $i = 1, 2$, chosen as in (24), (25) and $\lambda_i^\star$, $k_i^\star$ chosen as in Proposition 1, and the error attitude dynamics (28) controlled by (29) or, respectively, (30), with $k_p > 0$, $k_d > 0$, $\delta \in (0,\, 1)$ arbitrarily chosen. Then, the compact set*

$$\mathcal{A}^\star = \{(\tilde{\mathbf{p}}, \tilde{x}) \in \mathbb{R}^6 \times \mathcal{X}_{att} \,:\, \tilde{\mathbf{p}} = 0\,,\ \tilde{q} = h\mathbf{1}\,,\ \tilde{\omega}_c = 0\}$$

is globally asymptotically stable.

Proof: First, consider (28) controlled by (29). From Lemma 2, in the nominal case, the trajectories ω_c can be obtained as solutions to (38) and then Proposition 3 holds. Since the hybrid system (39) satisfies (A1)-(A3), from [23, Theorem 6.8] the hybrid system (39) is nominally well-posed and then [23, Lemma 7.8] implies that the compact set $\mathcal{A}$ in Proposition 3 is uniformly attractive from every compact set of the state space. Since $\mathcal{A}$ is stable, uniformly attractive from compact subsets of the state space, and, due to global asymptotic stability and by applying [23, Lemma 6.16], the reachable set from every given compact set is bounded, then [23, Lemma 7.11] implies that $\mathcal{A}$ is also $\mathcal{KL}$ asymptotically stable. As a consequence, for each maximal solution to (35), given $\Delta > 0$ there exists $T_\Delta > 0$ such that $\Theta(\mathcal{R}(\tilde{q}(t,j))) \leq \Delta$ for all $t + j \geq T_\Delta$, $(t,j) \in \operatorname{dom} \tilde{x}$. Hence, in finite time, $\Theta(\mathcal{R}(\tilde{q}))$ is arbitrarily small and, asymptotically, $\tilde{q} = h\mathbf{1}$ and $\tilde{\omega}_c = 0$. Now consider (28) controlled by (30). From Proposition 2, the same result holds following the same arguments employed above. By focusing now on the position error dynamics (21), it follows that, by choosing Δ sufficiently small, restrictions R_Δ on the exogenous input $\Gamma(R_c, R)$ given Proposition 1 are fulfilled in finite time and $\Gamma(R_c, R)$ approaches zero asymptotically. Then, since system (21) is a continuous-time system and it has no finite escape time, the result follows applying cascade control arguments as in [20, Corollary B.3.3]. In particular, for all $0 \leq t \leq T_\Delta$ solutions to (21) are defined and, since for all $t \geq T_\Delta$ the restrictions on the inputs are satisfied, $|\tilde{\mathbf{p}}|_a \leq \gamma_p |\Gamma|_a$ for some class-$\mathcal{K}$ function γ_p, which, since $|\Gamma_a| = 0$, implies that $\tilde{\mathbf{p}}$ converges to zero. □

Remark 3 *Note that the fact that the compact set $\mathcal{A}^\star$ in Proposition 4 is globally asymptotically stable implies that the position and the attitude of system (2) converge to the desired references (6), globally with respect to the initial conditions. This result, which overcomes the topological obstruction of globally stabilizing systems on manifolds via continuous feedback laws [24], takes advantage from the methodology proposed in [22] in which a globally stabilizing attitude controller is proposed.*

Remark 4 *The result in Proposition 4 for the overall closed-loop system does not require additional conditions on the tuning of the position and attitude controllers other than to the ones given in Propositions 1, 2 and 3. This useful property is obtained by designing the attitude controller in (29) (and (30)) so as to decouple (partially decouple) the inner attitude loop from the outer position loop. As a main limitation, the resulting attitude controller relies on the perfect knowledge of the system dynamics (in particular, see the feedforward terms (31) and (32)) and then it may not be robust to large uncertainties or exogenous disturbances.*

D. Attitude Stabilization: the Robust Case

Let us focus now on the general case in which the exogenous disturbances d_f and d_τ affect system (2) and just the nominal value J_0 of the inertia matrix J is available for feedback.

In this case it is possible to define the new attitude error coordinates

$$\tilde{q} := q_c^{-1} \otimes q, \quad \tilde{\omega}^* := \omega - \bar{\omega}^* \tag{40}$$

with $\bar{\omega}^* = R(\tilde{q})^\top \omega^*$. By bearing in mind (2) and (5), the

choice (40) leads to an attitude error dynamics of the form

$$\begin{aligned}\dot{\tilde{q}} &= \frac{1}{2}\tilde{q}\otimes\begin{bmatrix}0\\ \tilde{\omega}^*\end{bmatrix}-\frac{1}{2}\tilde{q}\otimes\begin{bmatrix}0\\ R(\tilde{q})^\top y_\zeta\end{bmatrix}\\ J\dot{\tilde{\omega}}^* &= \Sigma(\tilde{\omega}^*,\,\bar{\omega}^*)\,\tilde{\omega}^*+S(J\bar{\omega}^*)\bar{\omega}^*-JS(\mathcal{R}(\tilde{q})^\top y_\zeta)\,\bar{\omega}^*\\ &\quad -J\mathcal{R}(\tilde{q})^\top\dot{\omega}^*+u_\tau+d_\tau\end{aligned}\tag{41}$$

in which $y_\zeta := \omega_c-\omega^*$ and where $\Sigma(\tilde{\omega}^*,\,\bar{\omega}^*)$ is the skew-symmetric matrix defined just after (28) with $(\tilde{\omega}_c,\,\bar{\omega}_c)$ replaced by $(\tilde{\omega}^*,\,\bar{\omega}^*)$. As above, $\tilde{\eta}$ and $\tilde{\epsilon}$ denote respectively the scalar and vector part of the error quaternion $\tilde{q}$. Regarding the term y_ζ in (41) note that, by using the properties in Lemma 1, the following holds

$$y_\zeta := \Omega_1(\tilde{\mathbf{p}},t)-\omega^*(t)+\Omega_2(\tilde{\mathbf{p}},t)\,\Gamma(R,R_c)+\Omega_2(\tilde{\mathbf{p}},t)\,d_f(t)$$

where $\Omega_1(\tilde{\mathbf{p}},t)-\omega^*(t)$ and $\Omega_2(\tilde{\mathbf{p}},t)\,\Gamma(R,R_c)$ are bounded smooth functions vanishing respectively with $\tilde{\mathbf{p}}$ and $\tilde{\epsilon}$. Namely, $y_\zeta = y_\zeta(\tilde{\mathbf{p}},\tilde{\epsilon},d_f,t)$ with $y_\zeta(0,0,0,t)=0$. Furthermore, with the expression of $u^*_{\tau 0}$ in (11) at hand, note that the term $S(J\bar{\omega}^*)\bar{\omega}^*-J\mathcal{R}(\tilde{q})^\top\dot{\omega}^*$ in the last equation of (41) can be expressed as

$$\begin{aligned}&S(J\bar{\omega}^*)\bar{\omega}^*-J\mathcal{R}(\tilde{q})^\top\dot{\omega}^* =\\ &\qquad -u^*_{\tau 0}+\Delta_{1\omega}(\tilde{q},t)\,\tilde{\epsilon}+\Delta_{2\omega}(\tilde{q},t)\,(J-J_0)\end{aligned}$$

where $\Delta_{1\omega}$ and $\Delta_{2\omega}$ are smooth functions of appropriate dimension such that

$$\begin{aligned}\Delta_{1\omega}(\tilde{q},t)\tilde{\epsilon} &= J_0(I_3-\mathcal{R}(\tilde{q})^\top)\dot{\omega}^*+S(J_0\bar{\omega}^*)\bar{\omega}^*+\\ &- S(J_0\omega^\star)\omega^*,\\ \Delta_{2\omega}(\tilde{q},t)(J-J_0) &= (S(J\bar{\omega}^*)-S(J_0\bar{\omega}^*))\bar{\omega}^*+\\ &+ (J_0-J)\mathcal{R}(\tilde{q})^\top\dot{\omega}^*.\end{aligned}$$

Note that $\Delta_{i\omega}$, $i\in\{1,\,2\}$, are uniformly bounded, namely there exists a constant $\bar{\Delta}_\omega$ such that for all $\tilde{q}\in\mathbf{S}_3$ and $t\geq 0$

$$|\Delta_{i\omega}(\tilde{q},t)|\leq\bar{\Delta}_\omega\,,\quad i\in\{1,\,2\}\,.$$

Furthermore, note that

$$\omega^*\equiv 0\,,\ \dot{\omega}^*\equiv 0\ \Rightarrow\ \Delta_{2\omega}(\tilde{q},t)\equiv 0\,.\tag{42}$$

System (41) is thus a system driven by control input u_τ and affected by the exogenous disturbances $(d_f,d_\tau,\tilde{\mathbf{p}},(J_0-J)[\omega^*,\,\dot{\omega}^*])$. For this system, the attitude controller is selected as

$$u_\tau = u^*_{\tau 0}+u_{\tau,FB}(\tilde{q},\tilde{\omega}^*,h)\tag{43}$$

where the feedback law $u_{\tau,FB}$ is chosen as

$$u_{\tau,FB}(\tilde{q},\tilde{\omega}^*,h) \;=\; -k_p\,h\,\tilde{\epsilon}-k_p\,k_d\,\tilde{\omega}^*\tag{44}$$

in which k_p, k_d are positive gains and where $h\in\{-1,\,1\}$ is governed by the following hybrid dynamics

$$\begin{cases}\dot{h}=0 & h\,\tilde{\eta}\geq-\delta\ \text{ or }\ \tilde{\epsilon}^\top J^U\tilde{\epsilon}+\tilde{\omega}^{*\top}J^U\tilde{\omega}^*\geq 2k_d\,\delta\\ h^+\in\overline{\text{sgn}}(\tilde{\eta}) & h\,\tilde{\eta}\leq-\delta,\ \tilde{\epsilon}^\top J^U\tilde{\epsilon}+\tilde{\omega}^{*\top}J^U\tilde{\omega}^*\leq 2k_d\,\delta\end{cases}\tag{45}$$

with $\delta\in(0,1)$ and with the function $\overline{\text{sgn}}(\cdot)$ defined as Section IV-B. Note that, compared to (34), jumps occur only for sufficiently small values of the angular position and velocity errors. The whole attitude error system is thus a hybrid system of the form

$$\mathcal{H}_{\text{rob}}\ \begin{cases}\dot{\tilde{x}} &= F_{\text{rob}}(\tilde{x},\mathbf{d}) & \tilde{x}\in C_{\text{rob}}\\ \tilde{x}^+ &\in G_{\text{rob}}(\tilde{x}) & \tilde{x}\in D_{\text{rob}}\end{cases}\tag{46}$$

with $\tilde{x}=\text{col}(\tilde{q},\,\tilde{\omega}^*,\,h)$, $\mathbf{d}=\text{col}(d_f,d_\tau,\tilde{\mathbf{p}},(J_0-J)\omega^\star,(J_0-J)\dot{\omega}^\star)$, $F_{\text{rob}}(\cdot)$ is the vector given by the right-hand side of (41), $G_{\text{rob}}(\cdot)$ is defined as G_{nom} in the previous section, and

$$\begin{aligned}C_{\text{rob}} &= \{\tilde{x}\in\mathcal{X}_{att}\ :\ h\,\tilde{\eta}\geq-\delta\,\}\cup\\ &\quad\{\tilde{x}\in\mathcal{X}_{att}\ :\ \tilde{\epsilon}^\top J^U\tilde{\epsilon}+\tilde{\omega}^{*\top}J^U\tilde{\omega}^*\geq 2k_d\,\delta\}\\ D_{\text{rob}} &= \{\tilde{x}\in\mathcal{X}_{att}\ :\ h\,\tilde{\eta}\leq-\delta\,,\\ &\quad\tilde{\epsilon}^\top J^U\tilde{\epsilon}+\tilde{\omega}^{*\top}J^U\tilde{\omega}^*\leq 2k_d\,\delta\}\end{aligned}$$

It turns out that, if the inputs $(d_f,d_\tau,(J_0-J)\omega^*,(J_0-J)\dot{\omega}^*)$ are bounded, the design parameters can be tuned so as, after a finite amount of jumps, system (41) flows only and the resulting continuous-time system is characterized by an arbitrarily small asymptotic gain with respect to the input $\mathbf{d}$. This fact is formalized in the next Theorem.

Theorem 1 *Consider the hybrid system $\mathcal{H}_{\text{rob}}$ in (46). Let $\delta\in(0,1)$ and*

$$|d_f|_\infty\leq R_f,\quad |d_\tau|_\infty\leq R_\tau,\quad |(J-J_0)[\omega^*,\dot{\omega}^*]|_\infty\leq R_W\tag{47}$$

for some constants $R_f>0$, $R_\tau>0$ and $R_W>0$. For any $\gamma_{\text{att}}>0$, $c>0$, there exists $k_d^\star>0$ and for all $k_d\leq k_d^\star$ there exists $k_p^\star>0$ such that for all $k_p\geq k_p^\star$ and for all $\tilde{x}(0,0)\in C_{\text{rob}}\cup D_{\text{rob}}$ each maximal solution $\tilde{x}$ is complete and such that

- *there exists $T^\star>0$ such that $\tilde{x}(t,j)\in C_{\text{rob}}$ and $|\tilde{\epsilon}(t,j)|\leq c$ for all $(t,j)\in\text{dom}\,\tilde{x}$ such that $t+j\geq T^\star$;*
- $$\begin{aligned}\limsup_{t\to\infty}|\tilde{x}(t,j^\star)| &\leq \gamma_{\text{att}}\,\max\{|\tilde{\mathbf{p}}|_a\,,\,|d_f|_a\,,\,|d_\tau|_a\,,\\ &\qquad |J-J_0||[\omega^*,\dot{\omega}^*]|_a\}\end{aligned}$$

  where $j^\star=\sup\{j\ :\ (t,j)\in\text{dom}\,\tilde{x}\}$.

Proof: By the expression of ω_c and the properties of $\Omega_1(\cdot)$ and $\Omega_2(\cdot)$ in Lemma 1, by the fact that $\Gamma(R_c,R)$ is a smooth function vanishing at $\tilde{\epsilon}=0$, and by the definition of y_ζ, it turns out that there exist smooth matrices $\Delta_{i\eta}(\tilde{\mathbf{p}},\tilde{q},t)$ and $\Delta_{i\epsilon}(\tilde{\mathbf{p}},\tilde{q},t)$, $i=1,2,3$, of appropriate dimension such that

$$\begin{aligned}\frac{1}{2}\tilde{q}\otimes\begin{bmatrix}0\\ R(\tilde{q})^\top y_\zeta\end{bmatrix} &= \begin{bmatrix}\tilde{\epsilon}^\top\Delta_{1\eta}(\tilde{\mathbf{p}},\tilde{q},t)\\ \Delta_{1\epsilon}(\tilde{\mathbf{p}},\tilde{q},t)\end{bmatrix}\tilde{\epsilon}\\ &+\begin{bmatrix}\tilde{\epsilon}^\top\Delta_{2\eta}(\tilde{\mathbf{p}},\tilde{q},t)\\ \Delta_{2\epsilon}(\tilde{\mathbf{p}},\tilde{q},t)\end{bmatrix}+\begin{bmatrix}\tilde{\epsilon}^\top\Delta_{3\eta}(\tilde{\mathbf{p}},\tilde{q},t)\\ \Delta_{3\epsilon}(\tilde{\mathbf{p}},\tilde{q},t)\end{bmatrix}d_f\end{aligned}$$

and

$$|\Delta_{i\eta}(\tilde{\mathbf{p}},\tilde{q},t)|\leq\bar{\Delta}_q\,,\ \ |\Delta_{i\epsilon}(\tilde{\mathbf{p}},\tilde{q},t)|\leq\bar{\Delta}_q\,,\ \ i=1,2,3$$

for all $\tilde{\mathbf{p}}\in\mathbb{R}^6$, $\tilde{q}\in\mathbf{S}_3$, $t\geq 0$, where $\bar{\Delta}_q$ is a positive constant. Furthermore,

$$\Delta_{2\eta}(0,\tilde{q},t)=0\,,\quad\Delta_{2\epsilon}(0,\tilde{q},t)=0\quad\forall\,\tilde{q}\in\mathbf{S}_3\,,\ t\geq 0\,.$$

Moreover, there exist smooth matrices $\Delta_{i\omega}(\tilde{\mathbf{p}},\tilde{q},t), i=3,4,5$, of appropriate dimension such that

$$JS(\mathcal{R}(\tilde{q})^\top y_\zeta)\bar{\omega}^* = \Delta_{3\omega}(\tilde{\mathbf{p}},\tilde{q},t)\tilde{\epsilon}+\Delta_{4\omega}(\tilde{\mathbf{p}},\tilde{q},t)+\Delta_{5\omega}(\tilde{\mathbf{p}},\tilde{q},t)d_f$$

and $|\Delta_{i\omega}(\tilde{\mathbf{p}},\tilde{q},t)| \le \bar{\Delta}_\omega$, $i=3,4,5$, for all $\tilde{\mathbf{p}}\in\mathbb{R}^6$, $\tilde{q}\in\mathbf{S}_3$, $t\ge 0$, ω^* bounded, where $\bar{\Delta}_\omega$ is a positive constant. Furthermore, $\Delta_{4\omega}(0,\tilde{q},t)=0 \quad \forall\, \tilde{q}\in\mathbf{S}_3\,,\ t\ge 0$. By putting all the previous expressions in (41), along flows, the error attitude dynamics can be more explicitly rewritten as

$$\begin{aligned}
\dot{\tilde{\eta}} &= -\frac{1}{2}\tilde{\epsilon}^\top\tilde{\omega}^* + \tilde{\epsilon}^\top\Delta_{1\eta}(\cdot)\tilde{\epsilon}+\tilde{\epsilon}^\top d_\eta\\
\dot{\tilde{\epsilon}} &= \frac{1}{2}(\tilde{\eta}\tilde{\omega}^*+S(\tilde{\epsilon})\tilde{\omega}^*)+\Delta_{1\epsilon}(\cdot)\tilde{\epsilon}+d_\epsilon\\
J\dot{\tilde{\omega}}^* &= \Sigma(\cdot)\,\tilde{\omega}^*-u^\star_{\tau 0}+(\Delta_{1\omega}(\cdot)+\Delta_{3\omega}(\cdot))\tilde{\epsilon}+\Delta_{4\omega}(\cdot)\\
&\quad +\Delta_{5\omega}(\cdot)d_f+\Delta_{2\omega}(\tilde{q},\omega^*,\dot{\omega}^*)(J-J_0)+u_\tau+d_\tau
\end{aligned} \tag{48}$$

where

$$\begin{aligned}
d_\eta &= \Delta_{2\eta}(\tilde{\mathbf{p}},\tilde{q},t)+\Delta_{3\eta}(\tilde{\mathbf{p}},\tilde{q},t)d_f\\
d_\epsilon &= \Delta_{2\epsilon}(\tilde{\mathbf{p}},\tilde{q},t)+\Delta_{3\epsilon}(\tilde{\mathbf{p}},\tilde{q},t)d_f\,.
\end{aligned}$$

Let us define now the backstepping-like change of variable

$$\tilde{\omega}^* \ \mapsto\ \tilde{z}:=\tilde{\omega}^*+\frac{1}{k_d}h\,\tilde{\epsilon}$$

that transforms system (48) into

$$\begin{aligned}
\dot{\tilde{\eta}} &= -\frac{1}{2}\tilde{\epsilon}^\top\left(\tilde{z}-\frac{1}{k_d}h\,\tilde{\epsilon}\right)+\tilde{\epsilon}^\top\Delta_{1\eta}(\cdot)\tilde{\epsilon}+\tilde{\epsilon}^\top d_\eta\\
\dot{\tilde{\epsilon}} &= \frac{1}{2}(\tilde{\eta}I_3+S(\tilde{\epsilon}))\left(\tilde{z}-\frac{1}{k_d}h\,\tilde{\epsilon}\right)+\Delta_{1\epsilon}(\cdot)\tilde{\epsilon}+d_\epsilon\\
J\dot{\tilde{z}} &= \left(-k_pk_dI_3+\Sigma'_{k_d}(\tilde{z},\tilde{q},h)\right)\tilde{z}+\Sigma''_{k_d}(\tilde{z},\tilde{q},h)\tilde{\epsilon}+d_z
\end{aligned} \tag{49}$$

where

$$\begin{aligned}
\Sigma'_{k_d}(\cdot) &:= \Sigma(\cdot)+\frac{1}{2k_d}h\,(\tilde{\eta}I_3+S(\tilde{\epsilon}))\\
\Sigma''_{k_d}(\cdot)\tilde{\epsilon} &:= -\Sigma(\cdot)\frac{1}{k_d}\tilde{\epsilon}+(\Delta_{1\omega}(\cdot)+\Delta_{3\omega}(\cdot))\tilde{\epsilon}+\\
&\quad + \frac{1}{2k_d}hS(\tilde{\epsilon})\left(\tilde{z}-\frac{1}{k_d}h\tilde{\epsilon}\right)+\frac{1}{k_d}h\Delta_{1\epsilon}\tilde{\epsilon}\\
d_z &:= \left(\frac{J}{k_d}h\Delta_{2\epsilon}(\cdot)+\Delta_{4\omega}(\cdot)\right)+\\
&\quad + \left(\frac{J}{k_d}h\Delta_{3\epsilon}(\cdot)+\Delta_{5\omega}(\cdot)\right)d_f+\\
&\quad + \Delta_{2\omega}(\tilde{q},\omega^*,\dot{\omega}^*)(J-J_0)+d_\tau\,.
\end{aligned}$$

In order to study the asymptotic properties of system (46), consider the following candidate Lyapunov function

$$V(\tilde{x})=2(1-h\tilde{\eta})+\frac{1}{2}\tilde{z}^\top J\tilde{z}\,.$$

During flows, the time derivative of V reads as

$$\begin{aligned}
&\langle\nabla V(\tilde{x}),F_{\rm rob}(\tilde{x},\mathbf{d})\rangle =\\
&=-\frac{1}{k_d}\,\tilde{\epsilon}^\top\,\tilde{\epsilon}-\tilde{z}^\top\left(k_p\,k_dI_3-\Sigma'_{k_d}(\tilde{z},\tilde{q},h)\right)\tilde{z}+\\
&+\tilde{\epsilon}^\top\Delta_{1\eta}(\tilde{\mathbf{p}},\tilde{q},t)\tilde{\epsilon}+h\tilde{\epsilon}^\top\tilde{z}+\tilde{z}^\top\Sigma''_{k_d}(\tilde{z},\tilde{q},h)\tilde{\epsilon}+\\
&+\tilde{z}^\top d_z+d_\epsilon\,.
\end{aligned}$$

Note that $|(d_\eta,d_\epsilon,d_z)|_\infty \le \bar{d}$ for some positive constant $\bar{d}$ dependent on R_f, R_τ, R_W. As a consequence, standard high-gain arguments for continuous time systems (see in particular [25, Chapter 10]) can be used to claim that for any $\ell_1>0$ there exist $k_d^\star>0$ and, for all $k_d\le k_d^\star$, $k_p^\star>0$ such that for all $k_p\ge k_p^\star$ the following holds

$$\left.\begin{aligned}
|(\tilde{\epsilon},\tilde{z})| &\ge \ell_1|(d_\eta,d_\epsilon,d_z)|\\
\tilde{x} &\in C_{\rm rob}
\end{aligned}\right\}\\
\Rightarrow \langle\nabla V(\tilde{x}),F_{\rm rob}(\tilde{x},\mathbf{d})\rangle \le -\gamma V(\tilde{x}) \tag{50}$$

for some positive constant γ.

Let us now analyze the behavior of V during jumps. By definition of $D_{\rm rob}$, during jumps $\mathrm{sgn}h\neq\mathrm{sgn}\tilde{\eta}$ which implies that $h^+=-h$. Hence, $\tilde{z}^+=\tilde{\omega}^{*+}+(1/k_d)h^+\tilde{\epsilon}^+=\tilde{\omega}^*-(1/k_d)h\tilde{\epsilon}$ by which, recalling also (4), the following holds

$$\begin{aligned}
&V(\xi)-V(\hat{x})=\\
&2(1-h^+\tilde{\eta})+\frac{1}{2}\tilde{z}^{+\top}J\tilde{z}^+-2(1-h\tilde{\eta})-\frac{1}{2}\tilde{z}^\top J\tilde{z}\\
&=4h\tilde{\eta}+\frac{1}{2}\left(\tilde{\omega}^*-\frac{1}{k_d}h\tilde{\epsilon}\right)^\top J\left(\tilde{\omega}^*-\frac{1}{k_d}h\tilde{\epsilon}\right)\\
&\quad -\frac{1}{2}\left(\tilde{\omega}^*+\frac{1}{k_d}h\tilde{\epsilon}\right)^\top J\left(\tilde{\omega}^*+\frac{1}{k_d}h\tilde{\epsilon}\right)\\
&=4h\tilde{\eta}-\frac{2}{k_d}h\tilde{\omega}^{*\top}J\tilde{\epsilon}\\
&\le -4\delta+\frac{2}{k_d}|\tilde{\omega}^{*\top}J\tilde{\epsilon}| \le -4\delta+\frac{1}{k_d}\left(\tilde{\omega}^{*\top}J^U\tilde{\omega}^*+\tilde{\epsilon}^\top J^U\tilde{\epsilon}\right)\\
&\le -2\delta
\end{aligned}$$

for all $\xi\in G_{\rm rob}(\tilde{x})$. Now let $c_1\le c$ be a positive constant such that $|\tilde{\epsilon}|\le c_1\Rightarrow|\tilde{\eta}|>\delta$ and let $\ell_2>0$ be such that

$$V(\tilde{x})\le\ell_2 \quad\Rightarrow\quad |(\tilde{\epsilon},\tilde{z})|\le c_1\,.$$

Furthermore, by bearing in mind (50), fix $\ell_1>0$ (and $k_d^\star$ and $k_p^\star$ accordingly) and $0<\ell_3<\ell_2$ so that

$$|(\tilde{\epsilon},\tilde{z})|\le\ell_1\bar{d} \quad\Rightarrow\quad V(\tilde{x})\le\ell_3\,.$$

In summary, for all d_f, d_τ, J, $t\mapsto p^*(t)$, $t\mapsto\omega_z^*(t)$ such that $|d_f|_\infty\le R_f$, $|d_\tau|_\infty\le R_\tau$, $|J-J_0||[\omega^*,\dot{\omega}^*]|_\infty\le R_W$, and for all $\tilde{\mathbf{p}}\in\mathbb{R}^6$, we have that (50) holds and V is strictly decreasing during jumps. Accordingly, every complete solutions to $\mathcal{H}_{\rm rob}$ converge in finite time to the set $\mathcal{P}_{\ell 2}:=\{\tilde{x}\,:\,V(\tilde{x})\le\ell_2\}$.

Now, we show that every maximal solution to (46) is complete. From the fact that $\{\tilde{x}\,:\,V(\tilde{x})\le c'\}$ is compact for every $c'>0$, and, for all $\tilde{x}$ such that $V(\tilde{x})\ge\ell_2$, V is non increasing along solutions to (46), we have that solutions are bounded. Moreover the viability condition (VC) in [23, Proposition 6.10] holds for the hybrid system (46) with zero input, i.e., $\mathbf{d}\equiv 0$. Then, since $G_{\rm rob}(D_{\rm rob})\subset(C_{\rm rob}\cup D_{\rm rob})$ and, as shown above, from the fact that solutions are bounded, by applying [23, Proposition 6.10] it follows that all maximal solutions to (46) with zero input are complete. Since $G_{\rm rob}(D_{\rm rob})\cap D_{\rm rob}=\emptyset$ and the inputs d_f, d_τ, d_z in (49) are bounded, there is a finite (nonzero) amount of flows among jumps. This shows that every maximal solution to (46) in the presence of the input $\mathbf{d}$ satisfying (47) are complete. As a consequence, from (50), there exists a $T^\star>0$ such that

$V(\tilde{x}(t,j)) \leq \ell_2$ for all (t,j) in the hybrid time domain of the solution such that $t+j \geq T^\star$. Hence, by definition of c_1, $|\tilde{\epsilon}(t,j)| \leq |(\tilde{\epsilon}(t,j), \tilde{z}(t,j))| \leq c_1 < c$ for all (t,j) such that $t+j \geq T^\star$. This in particular implies that $\tilde{x}(t,j) \in C_{\rm rob}$ for all (t,j) such that $t+j \geq T^\star$, from which item 1 holds true. To prove item 2, note that for all $(t,j) \in \mathrm{dom}\,\tilde{x}$ such that $t+j \geq T^\star$ system (46) evolves as a continuous time system, namely no jumps occur. Accordingly, for all maximal solutions to (46), there exists $j^\star > 0$ such that $(t, j^\star)$ belong to $\mathrm{dom}\,\tilde{x}$ for all $t \geq T^\star$. The second item then follows by considering the continuous time system (49), the Lyapunov function (50), and by applying standard ISS arguments for continuous time systems [25, Chapter 10]. In particular the asymptotic bound involving $(J - J_0)[\omega^*, \dot{\omega}^*]$ follows from the property of $\Delta_{2\omega}(\cdot)$ in (42). □

Remark 5 *From the model inversion computed in Section III-B it follows that ω^*, $\dot{\omega}^*$ are functions of the position references $p^{*\,(3)}$, $p^{*\,(4)}$ and the attitude references ω_z^*, $\dot{\omega}_z^*$. Hence, the value of R_W in Theorem 1 depends on the desired position and attitude references and on the uncertainties on the inertia matrix J.*

Remark 6 *Theorem 1 shows how the attitude controller (43)-(45) is actually able to robustly globally stabilize the attitude error (40) in the presence of bounded exogenous disturbances and parametric uncertainties. This robustness property represents the main contribution of the proposed attitude control design with respect to the one proposed in [22]. Robust attitude controllers have appeared also in the space control literature (see [32] among others). The approach proposed in this work, however, is also able to overcome the topological obstruction using hybrid feedback control techniques so as to obtain a global property.*

E. Stability Properties of the Combined Position and Attitude Closed Loops in the Robust Case

By combining the claim of Theorem 1 and the one of Proposition 1, small gain arguments for continuous time systems can be used to conclude the asymptotic properties of the whole closed-loop system in the *robust case*. In fact, the following proposition holds true. [1]

Proposition 5 *Consider the whole closed-loop system given by the position error dynamics (21) controlled by (23), with λ_i and k_i, $i = 1, 2$, chosen as in (24), (25) and $\lambda_i^\star$, $k_i^\star$ chosen as in Proposition 1, and the error attitude dynamics (41) controlled by (43)-(45) with $\delta \in (0,\, 1)$. Let*

$$|d_f|_\infty \leq R_{d_f},\ |d_\tau|_\infty \leq R_{d_\tau},\ |(J - J_0)[\omega^*, \dot{\omega}^*]|_\infty \leq R_W$$

with R_{d_f} fixed by Proposition 1 and R_{d_τ}, R_W arbitrarily large positive numbers. Then there exists $k_d^\star > 0$ and, for all $k_d < k_d^\star$, $k_p^\star(k_d) > 0$ such that for all $k_p \geq k_p^\star(k_d)$ the following asymptotic bound holds true

$$|(\tilde{\mathbf{p}}, \tilde{\epsilon}, \tilde{\omega})|_a \leq \gamma \max\{|d_f|_a\,,\ \frac{1}{k_p}|d_\tau|_a,\ \frac{1}{k_p}|(J - J_0)[\omega^*,\, \dot{\omega}^*]|_a\}$$

for some $\gamma > 0$.

Proof: As a first step, note that there exists a positive constant $\bar{\Gamma}$ such that the $\Gamma(R_c, R)$ can be bounded as $|\Gamma(R_c, R)| \leq \bar{\Gamma}|\tilde{\epsilon}|$. With an eye to the statements of Proposition 1 and Theorem 1 , let $c > 0$ and $\gamma_{\rm att} > 0$ be fixed so that $\bar{\Gamma}\, c \leq R_\Gamma$ and

$$\gamma_{\rm att}\, \gamma_{\rm pos}\, \bar{\Gamma} < 1 \tag{51}$$

and let $k_d^\star$ and $k_p^\star$ fixed accordingly so that the properties of Theorem 1 are fulfilled with the restrictions on the inputs d_f, d_τ and $(J_0 - J)[\omega^*, \dot{\omega}^*]$ given by R_{d_f}, R_{d_τ} and R_W. Then, by Theorem 1, the restriction R_Γ on the input Γ of system (21) controlled by (23) is fulfilled in finite time. Moreover, there exists a time $T^\star$ such that for all $t + j \geq T^\star$ the closed-loop system flows only. At this point, asymptotic stability properties of the closed-loop system can be inferred by considering stability arguments for continuous-time systems. In particular, note that the small gain condition between the position and attitude subsystems is fulfilled by virtue of (51). The claimed asymptotic bound then follows from gain composition using the fact that $\gamma_{\rm att}$ in Theorem 1 can be arbitrarily decreased by increasing k_p. □

By considering a possible employment in real-world applications, note that the robust attitude control strategy derived in Section IV-D presents a number of advantages with respect to the nominal one proposed in Section IV-B. On the one hand, from Theorem 1, the robust attitude controller can be tuned to deal explicitly with model uncertainties and exogenous disturbances. The importance of such robustness will be also emphasized in Section V, in which the problem of controlling a prototype of quadrotor aerial vehicle is considered. Moreover, the robust attitude controller relies only on a simple feedback law (44) which depends on the actual state of the system and on the nominal model inversion computed in Section III-B. All of the above features thus suggest that the robust control strategy can be successfully employed in the design of an autopilot for VTOL aerial vehicles. As far as the stability of the overall position and attitude closed-loop system is concerned, note that the robust control strategy requires the attitude controller to be sufficiently fast (see the conditions on the attitude control parameters given in Proposition 5). This is a consequence of the fact that, in the *robust case*, it is not possible to decouple the position and the attitude dynamics trough a suitable design of the control torque as it has been done in the two solutions proposed for the *nominal case*.

Remark 7 *When a hybrid controller is subjected to measurement noise, multiple jumps or chattering may occur [23, Chapter 4]. This phenomenon may happen when jumps map the state back to the jump domain, namely $G(D) \cap D \neq \emptyset$. With an eye on (35) and (36), since $\delta > 0$, it follows*

[1] Hereafter, for the hybrid system $\mathcal{H}_{\rm rob}$, we compactly denote $|\phi|_a = \limsup_{(t,j) \in \mathrm{dom}\,\phi,\, t+j \to \infty} |\phi(t,j)|$.

that $G_{\rm nom}(D_{\rm nom}) \cap D_{\rm nom} = \emptyset$ (see [22, Subsection IV.E]). Moreover, with an eye on (46), since $G_{\rm rob} = G_{\rm nom}$ and $D_{\rm rob} \subset D_{\rm nom}$, it also holds that $G_{\rm rob}(D_{\rm rob}) \cap D_{\rm rob} = \emptyset$. As shown in [22, Subsection IV.E], the parameter δ can be also tuned to ensure robustness to possibly large measurement noise.

V. Application to the Control of a Quadrotor Aerial Vehicle

The control strategy developed for the *robust case* has been tested on a real quadrotor aerial vehicle. The selected prototype, which is depicted in Figure 2, is based on a carbon fiber tubular airframe characterized by high stiffness and low weight (about 220 grams). The prototype is actuated by four fixed-pitch propellers, each one driven by a brushless DC (BLDC) electric motor. The selected motors (Dualsky XM-400, 130 W of maximum power) and propellers (APC, 8 inches diameter) are able to produce approximately 2 Kg of total thrust when using a $3S$ LiPo (Lithium Polimery) battery as the poser source.

Fig. 2. Quadrotor prototype

Following [7], the dynamics of the system can be described by means of (2) in which the resultant force and torques can be computed as a function of the four thrusts T_i, $i = 1, 2, 3, 4$, generated by the four different propellers, namely

$$\begin{bmatrix} u_f \\ u_\tau \end{bmatrix} = \begin{bmatrix} -1 & -1 & -1 & -1 \\ 0 & -d & 0 & d \\ d & 0 & -d & 0 \\ K_{tm} & -K_{tm} & K_{tm} & -K_{tm} \end{bmatrix} \begin{bmatrix} T_1 \\ T_2 \\ T_3 \\ T_4 \end{bmatrix} \tag{52}$$

where d denotes the distance of the propeller spin axis from the center of gravity of the system, K_{tm} is a parameter which relates the thrust of a single motor to the aerodynamic torque produced along the spin axis of the propeller. The thrust T_i produced by each propeller is a function of the angular speed $\omega_{P,i}$ of the motors, namely $T_i = k_T \omega_{P,i}^2$, with $i \in \{1, 2, 3, 4\}$. The parameters of the specific prototype are $M = 1.05\ Kg$, $J_0 = \text{diag}(0.0082, 0.0082, 0.0164)\ Kg\,m^2$, $d = 0.29\ m$, and $K_{tm} = 0.026$. The values of K_{tm}, k_T, d and M have been measured experimentally with the help of a load-cell, while the value of the inertia J_0 has been estimated using a computer aided design software. To take into account possible uncertainties of the mass distribution, the following upper bound has been taken into account $J^U = \text{diag}(0.01, 0.01, 0.02)\ Kg\,m^2$.

With the above prototype at hand, the following two subsections propose respectively simulations and experimental results obtained by considering the robust control strategy defined in Sections IV-A and IV-D.

A. Simulations

Two different simulations are proposed. In the first one, the quadrotor is required to hover at a fixed position $p^\star$ starting from an initial attitude configuration in which the vehicle is overturned (attitude recovery maneuver). To govern the position dynamics, the controller (23) has been employed by choosing, according to Proposition 1, the control gains as $k_1^\star = 1$, $\lambda_1^\star = 5$, $k_2^\star = 150$, $\lambda_2^\star = 150$ and $\epsilon = 0.06$. For the attitude loop, the controller in (43), yielding robust global stability results, has been considered with $k_p = 40$, $k_d = 0.2$ and $\delta = 0.1$. To show the robustness of the proposed control law, realistic parametric uncertainties and disturbances have been considered in the simulations. In particular, the actual inertia J of the vehicle is assumed to be 10 % larger than the nominal one, while the forces and torques disturbances d_f and d_τ are selected as coloured noise with maximum amplitude of 1.5 N and 0.05 Nm, respectively, to model the effects of possible wind impacting propellers. Finally, a white noise with maximum amplitude of 0.04 rad has been added to the attitude position measurement to represent uncertainties in the sensor model.

Figures 3, 4 and 5 show the attitude position, the angular speed and the linear position of the vehicle during the attitude recovery maneuver. Note that, despite the vehicle in the initial position is overturned, i.e., $[\eta(0), \epsilon(0)^\top]^\top = [0, 1, 0, 0]^\top$, the vehicle converges rapidly to the desired hover configuration by rotating around the body x-axis. This is achieved without undesired switches of the hybrid state h, as depicted in Figure 6. This result may not be achieved with continuous time controllers having the above initial condition as equilibrium point, or with discontinuous feedback laws not robust to measurement noise (see also [33]). Finally, the force and torque control inputs applied to the quadrotor during the maneuver are depicted in Figure 7.

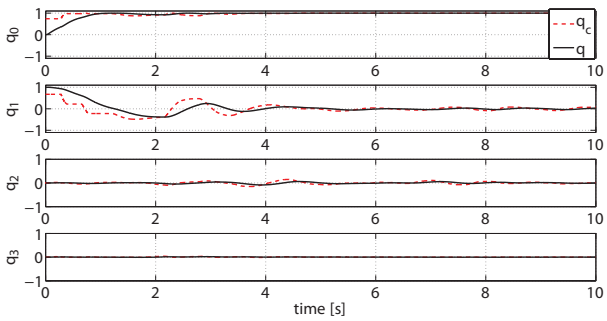

Fig. 3. The attitude trajectory of the quadrotor during the attitude recovery maneuver.

The second simulation considers an aggressive maneuver (barrel flip) to be accomplished by the vehicle. In particular, the desired time reference signals are given by $x^*(t) := 0$, $y^*(t) := \cos(\gamma t)$, $z^*(t) := -\sin(\gamma t)$, where $\gamma := 1.4\pi$ rad/s. In practice the quadrotor is required to follow a circular trajectory along the y and z inertial axis maintaining a constant speed along the path. The reference inputs u_f^* and u_τ^*, required to compute the feed-forward control terms in (15) and (43), have been computed as in Section III-A with R^* obtained using the algorithm in Appendix C. For the above reference

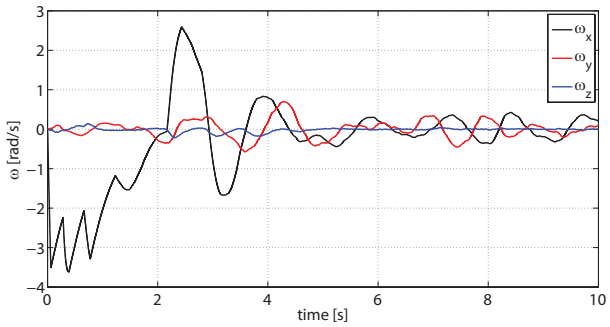

Fig. 4. The angular speed of the quadrotor during the attitude recovery maneuver.

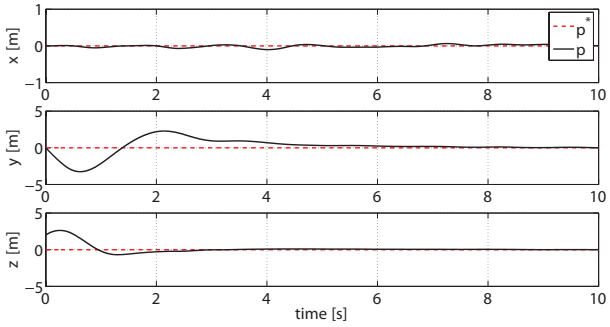

Fig. 5. The position trajectory of the quadrotor during the attitude recovery maneuver.

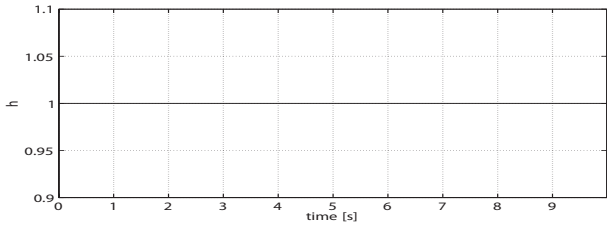

Fig. 6. The logic state h of the quadrotor during the attitude recovery maneuver.

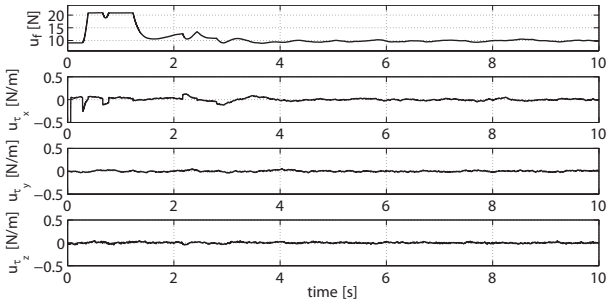

Fig. 7. The control force and torques applied to the quadrotor during the attitude recovery maneuver.

trajectory, condition (9) holds with $\epsilon \leq 0.1$. Thus the same position and attitude control parameters of the first simulation have been considered. The actual and the reference position trajectories are depicted in Figure 10, showing how the system converges to the desired path. Figure 8 shows the attitude of the vehicle during the aggressive maneuver and Figure 9 shows the angular velocity. Note that, to compensate for the high centrifugal force with the thrust forces generated by the propellers, the quadrotor has to continuously rotate around the body x axis.

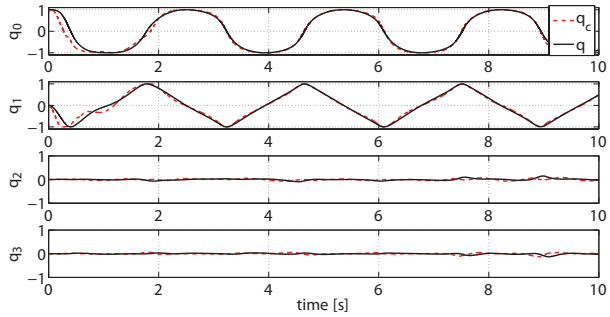

Fig. 8. The attitude trajectory of the quadrotor during the aggressive maneuver.

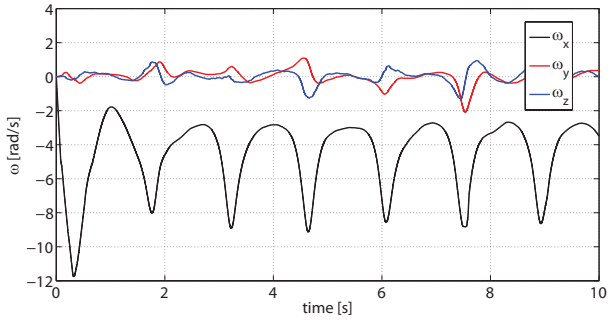

Fig. 9. The angular speed of the quadrotor during the aggressive maneuver.

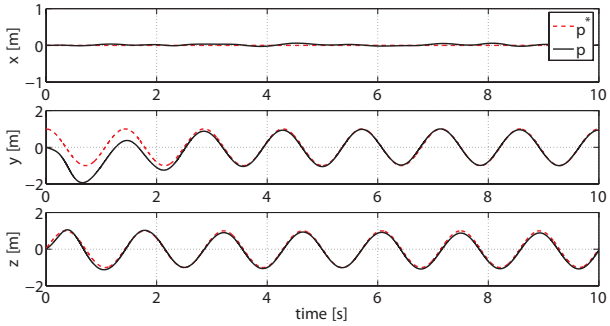

Fig. 10. The position trajectory of the quadrotor during the aggressive maneuver.

B. Experiments

The goal of this section is to show the performance of the proposed robust inner-outer loop control strategy in a real-world application scenario. In particular, the robust control strategy developed in Sections IV-A and IV-D has been implemented on a real autopilot [34] in order to stabilize the quadrotor prototype described in Section V. To determine the attitude of the vehicle, the selected autopilot includes an Inertial Measurement Unit (IMU) which consists of $3D$ accelerometers, magnetometers and gyros. The low-level sensor information obtained by the IMU is processed by an Attitude

and Heading Reference System (AHRS) algorithm, derived following [35], in order to compute the attitude quaternion and the angular speed of the system. An external motion tracking system [36] has then been employed to determine the linear position of the center of gravity of the vehicle. The selected motion tracking system is able to measure the position at 100 Hz with approximately 1 mm accuracy. With this information at hand, a standard high-gain observer [37, Chapter 14.5] has been employed to compute the linear velocities in real-time. All of the control and estimation algorithms run in real-time at 200 Hz rate on a 32 bit ARM processor. The parameters for the controller used in the experiment are: $k_1^\star = 1$, $\lambda_1^\star = 5$, $k_2^\star = 150$, $\lambda_2^\star = 150$, $\epsilon = 0.06$, $k_p = 16$, $k_d = 0.7$ and $\delta = 0.15$. The value of δ has been selected to take into account the measurement noise on attitude estimation of the specific prototype.

The goal of the proposed experiment is twofold. On the one hand, it shows how the proposed control strategy is actually effective in practical applications in which model uncertainties, disturbances and noises are present. On the other hand, it shows how the proposed global stabilizing controller is able to overcome typical limitations of some continuous-time stabilizing controllers, such as in particular the *un-winding* phenomenon [38]. In the experiment, the vehicle is deployed by the hand of a human operator and the controller is required to maintain a constant position and attitude. Due to this particular type of deployment, large initial attitude errors can be introduced since the vehicle may rotate when it is launched by the operator.

Figures[2] 12 and 13 show the attitude position and angular velocity of the vehicle during the experiment. Note that the vehicle starts close to the unit quaternion $q = [1, 0, 0, 0]^\top$ and then, due to manual deployment procedure, is rotated by approximately 2π around the body z axis. Note that at time $t \approx 3.9$ sec, η is close to zero while ϵ is close to $[0, 0, -1]^\top$. Due to this large attitude error, the jump domain D_{rob} in (46) is entered. Note that, due to the small values of the inertia J^U, the jump condition in (45) can be entered even when the vehicle is rotating at relative large angular speed values (up to 3 rad/s for the parameters employed in the experiments). Thus the logic state h, which is depicted in Figure 14, switches from 1 to -1 and the unit quaternion $q = [-1, 0, 0, 0]^\top$ is stabilized. This fact prevents the vehicle to perform a complete rotation around its body z axis in order to reach $q = [1, 0, 0, 0]^\top$, which, according to the Rodrigues formula, corresponds to the same orientation. The position of the vehicle during the maneuver has been depicted in Figure 11 while the control inputs are given in Figure 15. A video showing the experiment is available at https://www.youtube.com/watch?v=FFW2MchU79A.

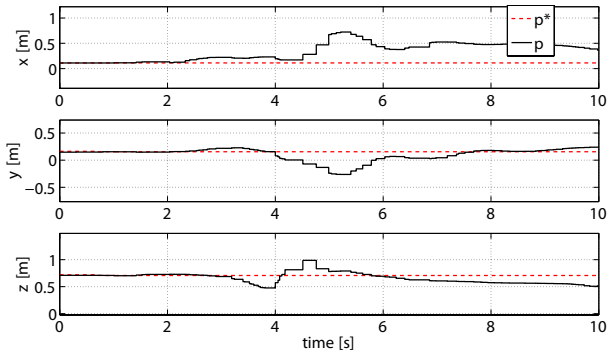

Fig. 11. Position during the hand deployment maneuver.

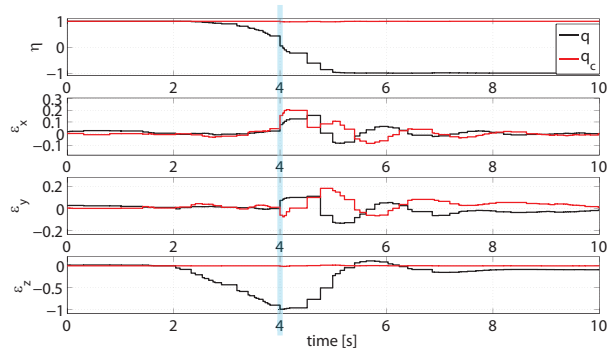

Fig. 12. Attitude quaternion during the hand deployment maneuver. Between time $t = 2s$ and $t \simeq 4s$ the quadrotor is forced to a rotation around z axis by the human operator. At time $t \simeq 4s$ the quadrotor is deployed.

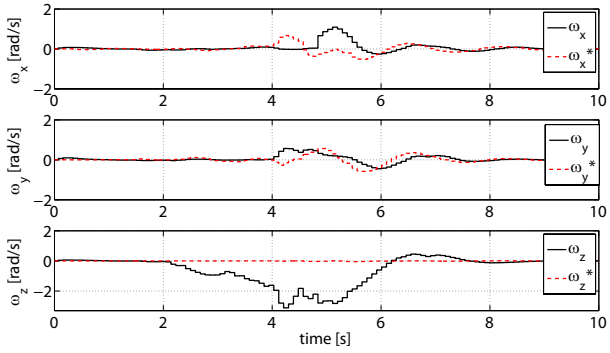

Fig. 13. Angular speed during the hand deployment maneuver.

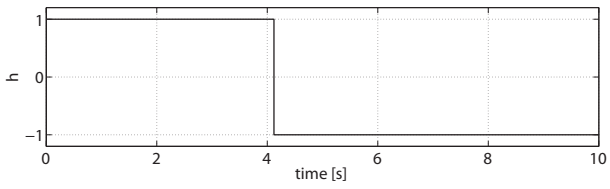

Fig. 14. The logic state h during the hand deployment maneuver.

VI. Conclusions

Control strategies to let the dynamics of a class of VTOL aerial vehicles tracking a desired position and attitude trajectory globally with respect to the initial conditions have been presented. The proposed feedback controllers are based on a hierarchical control paradigm in which the attitude, which is governed by means of a hybrid controller so as to overcome the well-known topological constraint, is employed as a virtual input to stabilize the aircraft position. Two main approaches have been proposed and compared. The first one is based on the idea of decoupling the attitude from the position dynamics

[2]Measurements are obtained from the onboard autopilot at 10 Hz rate.

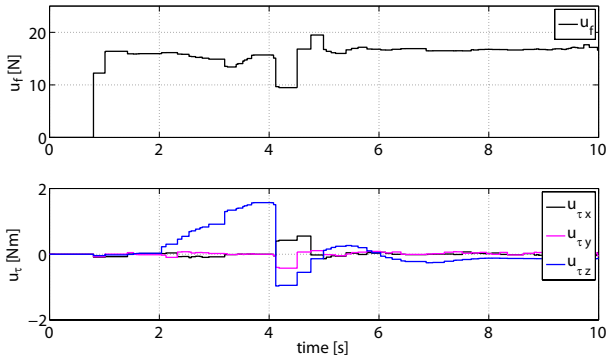

Fig. 15. The force and torques control inputs applied to the aerial vehicle during the hand deployment maneuver.

by taking into account perfect knowledge of the dynamical model of the system. The second approach, on the other hand, aims at obtaining a controller which is robust with respect to the presence of uncertainties and exogenous disturbances such as wind gusts. Since the dynamical model of the system is not perfectly known, the position and attitude dynamics cannot be decoupled. Hence the stability analysis requires to deal with the feedback interconnection between the hybrid attitude and the continuous-time position closed-loop subsystems. The resulting controller is characterized by a very simple structure, i.e., by a linear error feedback term driven by the logic required to overcome the topological obstruction and a feedforward term deriving from the references to be tracked. Simulations and experiments obtained considering a prototype of quadrotor aerial vehicle finally show how the robust controller can be effectively employed in practical applications.

REFERENCES

[1] E. Feron and E.N. Johnson. Aerial robotics. In B. Siciliano and O. Khatib, editors, *Springer Handbook of Robotics*, pages 1009–1027. Springer, 2008.

[2] A. Bachrach, R. He, and N. Roy. Autonomous flight in unknown indoor environments. *International Journal of Micro Air Vehicles*, 1(4):217–228, 2009.

[3] L. Marconi and R. Naldi. Control of aerial robots. hybrid force/position feedback for a ducted-fan. *IEEE Control System Magazine*, 32(4):43–65, 2012.

[4] V. Gavrilets, E. Frazzoli, B. Mettler, M. Piedimonte, and E. Feron. Aggressive maneuvering of small autonomous helicopters: A human-centered approach. *The International Journal of Robotics*, 20(10):795–807, 2001.

[5] J.M. Pflimlin, P. Soueres, and T. Hamel. Hovering flight stabilization in wind gusts for ducted fan UAV. *42nd IEEE Conf. on Decision and Control*, 2004.

[6] R. Naldi, L. Gentili, L. Marconi, and A. Sala. Design and experimental validation of a nonlinear control law for a ducted-fan miniature aerial vehicle. *Control Engineering Practice*, 18(7):747–760, 2010.

[7] P. Pounds, R. Mahony, and P. Corke. Modelling and control of a large quadrotor robot. *Control Eng. Pract.*, 18(7):691–699, 2010.

[8] S. Bouabdallah and R. Siegwart. *Advances in Unmanned Aerial Vehicles*, chapter Chapter 6: Design and Control of a Miniature Quadrotor, pages 171–210. Springer Press, Feb. 2007.

[9] R. Cunha, D. Cabecinhas, and C. Silvestre. Nonlinear trajectory tracking control of a quadrotor vehicle. In *Proc. European Control Conference*, 2009.

[10] J. Hauser, S. Sastry, and G. Meyer. Nonlinear control design for slightly non-minimum phase systems: application to V/STOL aircraft. *Automatica*, 28(4):665–679, 1992.

[11] P. Martin, S. Devasia, and B. Paden. A different look at output tracking: control of a VTOL aircraft. *Automatica*, 32(1):101–107, 1996.

[12] T. Koo and S. Sastry. Output tracking control design of a helicopter model based on approximate linearization. In *Decision and Control, 1998. Proceedings of the 37th IEEE Conference on*, volume 4, pages 3635–3640 vol.4, Dec 1998.

[13] R. Mahony and T. Hamel. Robust trajectory tracking for a scale model autonomous helicopter. *Int. J. Robust Nonlinear Control*, 14:1035–1059, 2004.

[14] M.D. Hua, T. Hamel, P. Morin, and C. Samson. A control approach for thrust-propelled underactuated vehicles and its applications to VTOL drones. *IEEE Transsactions on Automatic Control*, 54(8):1837–1853, 2009.

[15] A. Abdessameud and A. Tayebi. Global trajectory tracking control of VTOL-UAVs without linear velocity measurements. *Automatica*, 46(4):1053–1059, April 2010.

[16] T. Lee, M. Leok, and N.H. McClamroch. Nonlinear robust tracking control of a quadrotor UAV on SE(3). *Asian Journal of Control*, 15(3):1–18, May 2013.

[17] E. Frazzoli, M. Dahleh, and E. Feron. Trajectory tracking control design for autonomous helicopters using a backstepping algorithm. *Proceedings of the American Control Conference*, pages 4102–4107, 2000.

[18] P. Casau, R.G. Sanfelice, R. Cunha, D. Cabecinhas, and C. Silvestre. Global trajectory tracking for a class of underactuated vehicles. In *Proceedings of American Control Conference*, pages 419–424, Washington DC, US, 2013.

[19] L. Marconi and R. Naldi. Robust nonlinear full degree of fredom control of an helicopter. *Automatica*, 42:1584–1596, 2007.

[20] A. Isidori, L. Marconi, and A. Serrani. *Robust Autonomous Guidance: An Internal Model Approach*. Advances in Industrial Control. Springer-Verlag London, 2003.

[21] M. Hua, T. Hamel, P. Morin, and C. Samson. Introduction to feedback control of underactuated VTOL vehicles. *IEEE Control Systems Magazine*, 33(2):61–75, February 2013.

[22] C.G. Mayhew, R.G. Sanfelice, and A.R. Teel. Quaternion-based hybrid controller for robust global attitude tracking. *IEEE Transactions on Automatic Control*, 56(11):2555–2566, November 2011.

[23] R. Goebel, R. G. Sanfelice, and A. R. Teel. *Hybrid Dynamical Systems Modeling, Stability, and Robustness*. Princeton University Press, 2012.

[24] S.B. Bhat and D.S. Bernstein. A topological obstruction to continuous global stabilization of rotational motion and the unwinding phenomenon. *System & Control Letters*, 39:63–70, 1999.

[25] A. Isidori. *Nonlinear Control Systems II*. Springer Verlag London, 1999.

[26] M.D. Shuster. A survey of attitude representation. *The Journal of the Astronautical Sciences*, 41(4):439–517, December 1993.

[27] A. Teel. A nonlinear small gain theorem for the analysis of control systems with saturations. *IEEE Transactions on Automatic Control*, 41:1256–1270, 1996.

[28] D. Angeli, Y. Chitour, and L. Marconi. Robust stabilization via saturated feedback. *IEEE Transactions on Automatic Control*, 50(12):1997 – 2014, 2005.

[29] W. Liu, Y. Chitour, and E.D. Sontag. On finite gain stabilization of linear systems subject to input saturation. *SIAM J. Control Optim.*, 34:1190 – 1219, 1996.

[30] C. Mayhew, R. Sanfelice, and A. Teel. On path-lifting mechanisms and unwinding in quaternion-based attitude control. *IEEE Transactions on Automatic Control*, 58(5):1179–1191.

[31] R.G. Sanfelice, R. Goebel, and A.R. Teel. Invariance principles for hybrid systems with connections to detectability and asymptotic stability. *IEEE Transactions on Automatic Control*, 52(12):2282–2297, 2007.

[32] Z. Chen and J. Huang. Attitude tracking and disturbance rejection of rigid spacecraft by adaptive control. *Automatic Control, IEEE Transactions on*, 54(3):600–605, March 2009.

[33] E. Garone, R. Naldi, and E. Frazzoli. Switching control laws in the presence of measurement noise. *Systems & Control Letters*, 59(6):353 – 364, 2010.

[34] L. Meier, P. Tanskanen, F. Fraundorfer, and M. Pollefeys. Pixhawk: A system for autonomous flight using onboard computer vision. In *Robotics and Automation (ICRA), 2011 IEEE International Conference on*, pages 2992–2997, May 2011.

[35] J. Farrell. *Aided Navigation: GPS with High Rate Sensors*. Mc Graw Hill, 2008.

[36] Optitrack motion tracking system. www.naturalpoint.com/optitrack.

[37] H. K. Khalil. *Nonlinear systems*. Prentice Hall, 1996.

[38] J.T.-Y. Wen and K. Kreutz-Delgado. The attitude control problem. *Automatic Control, IEEE Transactions on*, 36(10):1148–1162, Oct 1991.

APPENDIX A
PROOF OF LEMMA 1

By the definition of R_c in (18), (20) and using $R_c^\top \dot{R}_c e_3 = S(\omega_c)e_3$ it follows that

$$\omega_c = \bar{G}\, R_c^\top \frac{d}{dt}\frac{v_c(\tilde{\mathbf{p}},t)}{|v_c(\tilde{\mathbf{p}},t)|} + \omega_z^* e_3$$

in which $\bar{G} \in \mathbb{R}^{3\times 3}$ is the matrix with the first, second and third rows given by $[0,\,-1,\,0]$, $[1,\,0,\,0]$ and $[0,\,0,\,0]$, respectively, and

$$\frac{d}{dt}\frac{v_c}{|v_c|} = \left(\frac{I_3}{|v_c|} - \frac{v_c v_c^\top}{|v_c|^3}\right)\left(\dot{v}_f^* + \dot{\kappa}(\tilde{\mathbf{p}})\right) .$$

By taking advantage from the nested saturation structure of $\kappa(\cdot)$ in [20] it is possible to show that $\dot{\kappa}(\cdot)$ is upper bounded by a value not dependent on $\tilde{\mathbf{p}}$. To this purpose, let $\zeta := \dot{\tilde{p}} + \lambda_1\sigma\left(k_1\tilde{p}/\lambda_1\right)$ so that $\kappa(\tilde{\mathbf{p}}) = \lambda_2\sigma(k_2\zeta/\lambda_2)$ and

$$\begin{aligned}\dot{\kappa}(\cdot) &= \frac{k_2}{M}\sigma'\left(\frac{k_2\zeta}{\lambda_2}\right)\left(-\lambda_2\sigma\left(\frac{k_2\zeta}{\lambda_2}\right)+\right.\\ &+ \left. Mk_1\sigma'\left(\frac{k_1\tilde{p}}{\lambda_1}\right)\dot{\tilde{p}} + \Gamma + d_f\right)\end{aligned}$$

from which the expressions of $\Omega_1(\cdot)$ and $\Omega_2(\cdot)$ immediately follow. The fact that $\Omega_1(0,t) = \omega^\star$ follows from (12) and $\sigma(0) = 0$. Finally, the fact that Ω_1 and Ω_2 are uniformly bounded by a constant $\bar{\Omega}$ follows from the fact that v_c, $\sigma(\cdot)$ and $\sigma'(\cdot)$ are bounded functions (by the definition of saturation function and by (15)), and that $\sigma'(k_2\zeta/\lambda_2)\dot{\tilde{p}}$ is a bounded term. As a matter of fact note that, in the computation of a bound for $\sigma'(k_2\zeta/\lambda_2)\dot{\tilde{p}}$, it is possible to assume $|\zeta| \le \lambda_2/k_2$ (otherwise $\sigma'(k_2\zeta/\lambda_2) = 0$ by the definition of saturation function) and thus, by the definition of ζ, $|\dot{\tilde{p}}| \le \sqrt{3}(\lambda_2 + \lambda_2/k_2)$. This completes the proof of the lemma.

APPENDIX B
PROOF OF LEMMA 2

From Lemma 1, since $d_f \equiv 0$ and Γ is bounded, we have that $\omega_c(t)$ is a bounded function of time. By computing the derivative of $\omega_c(t)$ we obtain

$$\dot{\omega}_c = \bar{G}S(\omega_c)^\top R_c^\top \frac{d}{dt}\frac{v_c}{|v_c|} + R_c^\top \frac{d^2}{dt^2}\frac{v_c}{|v_c|} + \dot{\omega}_z^\star e_3$$

where the expression of $(d/dt)(v_c/|v_c|)$ is given in the proof of Lemma 1, and it is bounded when $d_f \equiv 0$, while

$$\begin{aligned}\frac{d^2}{dt^2}\frac{v_c}{|v_c|} &= \left(\frac{-v_c v_c^\top}{|v_c|^3} - \frac{\dot{v}_c v_c^\top + v_c\dot{v}_c^\top - 3(v_c v_c^\top)^2}{|v_c|^5}\right)\dot{v}_c +\\ &+ \left(\frac{I_3}{|v_c|} - \frac{v_c v_c^\top}{|v_c|^3}\ddot{v}_c\right)\end{aligned}$$

with $\dot{v}_c = \dot{v}_f^\star + \dot{\kappa}(\cdot)$, $\ddot{v}_c = \ddot{v}_f^\star + \ddot{\kappa}(\cdot)$. From the assumptions on the references given in Section III-B and by considering the proof of Lemma 1 for the special case in which $d_f \equiv 0$, we have that $\ddot{v}_f^\star$ and $\dot{\kappa}(\cdot)$ are bounded functions of time. Then the result follows by showing that, when $d_f \equiv 0$, also $\ddot{\kappa}(\cdot)$ is bounded. Specifically, we have

$$\ddot{\kappa}(\cdot) = \frac{k_2^2}{\lambda_2}\sigma''\left(\frac{k_2\zeta}{\lambda_2}\right)\dot{\zeta}^2 + k_2\sigma'\left(\frac{k_2\zeta}{\lambda_2}\right)\ddot{\zeta}$$

with

$$\begin{aligned}\dot{\zeta} &= \frac{1}{M}\left(-\kappa(\cdot)+\Gamma\right) + k_1\sigma'\left(\frac{k_1\tilde{p}}{\lambda_1}\right)\dot{\tilde{p}}\\ \ddot{\zeta} &= -\frac{1}{M}\dot{\kappa}(\cdot) + \frac{1}{M}\dot{\Gamma} + \frac{k_1^2}{\lambda_1}\sigma''\left(\frac{k_1\tilde{p}}{\lambda_1}\right)\dot{\tilde{p}}^2 +\\ &+ k_1\sigma'\left(\frac{k_1\tilde{p}}{\lambda_1}\right)\ddot{\tilde{p}}.\end{aligned}$$

When $|\zeta| > k_2/\lambda_2$, from the definition of $\sigma(\cdot)$, we have that $\sigma'(k_2\zeta/\lambda_2) = \sigma''(k_2\zeta/\lambda_2) = 0$. In the other case, when $|\zeta| \le k_2/\lambda_2$, from the definition of ζ given in the proof of Lemma 1, we have that $|\dot{\tilde{p}}| \le \sqrt{3}(\lambda_2 + \lambda_2/k_2)$. Then, by considering also the definition of Γ given in (22) and $\ddot{\tilde{p}}$ given by (21) with $d_f \equiv 0$, since $\sigma(\cdot)$, $\sigma'(\cdot)$, $\sigma''(\cdot)$ are bounded functions, all terms in the expressions of $\dot{\zeta}$ and $\ddot{\zeta}$ are bounded. This proves the lemma.

APPENDIX C
COMPUTATION OF THE ROTATION MATRIX

A rotation matrix satisfying (8) (or equivalently (18)) can be obtained parameterizing rotations using Euler angles. In fact, given $\nu = [\nu_x,\,\nu_y,\,\nu_z]^\top \in S_2$, a matrix $R' \in SO(3)$ s.t. $R'e_3 = \nu$ can be obtained as (i) $R' = R_xR_yR_z$ or (ii) $R' = R_yR_xR_z$ with

$$\begin{aligned}R_x &= \begin{bmatrix}1 & 0 & 0\\ 0 & \cos\phi & -\sin\phi\\ 0 & \sin\phi & \cos\phi\end{bmatrix},\\ R_y &= \begin{bmatrix}\cos\theta & 0 & \sin\theta\\ 0 & 1 & 0\\ -\sin\theta & 0 & \cos\theta\end{bmatrix},\\ R_z &= \begin{bmatrix}\cos\psi & -\sin\psi & 0\\ \sin\psi & \cos\psi & 0\\ 0 & 0 & 1\end{bmatrix},\end{aligned}$$

where $\phi,\,\theta,\,\psi \in \mathbb{R}$. Since $R_ze_3 = e_3$ for all $\psi \in \mathbb{R}$, the value of ψ can be considered as a degree of freedom (namely the *heading direction* of the vehicle can be assigned arbitrarily) when R' is computed as in (i) or (ii). For the case (i), if $\nu_z \neq 0$ or $\nu_y \neq 0$, ϕ and θ can be obtained as

$$\phi = \arctan\left(\frac{-\nu_y}{\nu_z}\right),\ \theta = \text{asin}(\nu_x)\,.$$

When ν_z and ν_y are close to zero, since ν_x is different from zero from the definition of S_2, the expression of R' can be computed as in (ii) with ϕ and θ given as

$$\phi = \text{asin}(-\nu_y),\ \theta = \arctan\left(\frac{\nu_x}{\nu_z}\right) .$$